Climate Dynamics
https://doi.org/10.1007/s00382-018-4398-6

Short-term concurrent drought and heatwave frequency with 1.5 and 2.0 °C global warming in humid subtropical basins: a case study in the Gan River Basin, China

Yuqing Zhang[1,3] · Qinglong You[2,3] · Guangxiong Mao[1] · Changchun Chen[4] · Zhengwei Ye[1]

Received: 4 December 2017 / Accepted: 10 August 2018

Abstract
Short-term concurrent droughts and heatwaves accompanied by high temperatures and low soil moisture (or low precipitation) may significantly impact ecosystems, societies, and economies although the individual events involved may not themselves represent severe extremes. There is little known about the potential frequency of short-term concurrent droughts and heatwaves in the future. Here, we use the Gan River Basin as a case study area to assess the effects of different warming levels on drought and heatwave concurrences based on the coupled model intercomparison project phase 5 and variable infiltration capacity (VIC) model. The results show that the VIC model has high reliability in the simulation of soil moisture and evapotranspiration compared with other well-recognized datasets in the Gan River Basin. The warming level over the Gan River Basin is close to the global warming level. Under RCP4.5 and RCP8.5 scenarios, the multi-model ensemble medians of concurrent events increased by 0.08–0.4 pentads/decade from 2006 to 2099. The uncertainty of concurrent events encompasses a wider range as global temperature increases. Compared to the reference period (1961–2005), drought and heatwave concurrences have increased by more than 50% in the most parts of the basin under 1.5 or 2.0 °C of global warming; there is a 20% frequency difference of 0.5 °C from 1.5 to 2.0 °C. The substantial pentad increases (at least greater than 50%) existed in historical low-pentad-value areas in a 1.5 or 2.0 °C world, especially pronounced for a 2.0 °C world. The greatest increase in concurrent event pentads came from the 25th percentile values in 1.5 or 2.0 °C scenarios. Climatological median pentads of concurrent droughts and heatwaves appear likely to be 9.6–17.6% more frequent in a 2.0 °C world than a 1.5 °C world with respect to the reference period.

Keywords Concurrent droughts and heatwaves · 1.5 and 2.0 °C of global warming · Variable infiltration capacity (VIC) · Gan River Basin · China

1 Introduction

According to the Fifth Assessment Report (AR5) of the Intergovernmental Panel on Climate Change (IPCC), the frequency and intensity of many climate extremes have increased as a result of global warming over recent decades. These extremes are projected to continue in the future alongside continued warming (IPCC 2013). Concurrent sets of two or more climate extremes (e.g., high temperatures and low precipitation) can more significantly impact natural systems and societies compared to individual occurrences. Recent researchers have extensively studied concurrent droughts and heatwaves due to the increase of these events under global warming (Aghakouchak et al. 2015; Mazdiyasni and Aghakouchak 2015; Sharma and Mujumdar 2017).

✉ Qinglong You
yqingl@126.com

Yuqing Zhang
geonuist@foxmail.com

[1] School of Urban and Environmental Science, Huaiyin Normal University, Huai'an 223300, China

[2] Department of Atmospheric and Oceanic Sciences and Institute of Atmospheric Sciences, Fudan University, Shanghai 200433, China

[3] Key Laboratory of Meteorological Disaster, Ministry of Education (KLME)/Joint International Research Laboratory of Climate and Environment Change (ILCEC), Nanjing University of Information Science and Technology (NUIST), Nanjing 210044, China

[4] School of Geography and Remote Sensing, NUIST, Nanjing 210044, China

Published online: 14 August 2018

Flash droughts differ from traditional droughts (wherein below-average water availability persists for some amount of time) as they evolve rapidly, typically within crop growing seasons, and are characterized by the concurrence of high temperatures and low soil moisture (Otkin et al. 2013; Mo and Lettenmaier 2015). The rapid onset of a flash drought wreaks a devastating impact on society and economy, especially for agricultural crops (Mo and Lettenmaier 2015; Otkin et al. 2016; Paimazumder and Done 2016). Although there is no universally accepted definition of "flash drought", two basic concepts are relevant: the rate of intensification (defining the degree of rapidity as "flash") and the water deficit (defining the "drought").

Flash droughts have received significant research attention in recent years (Ford et al. 2015; Mo and Lettenmaier 2015, 2016; Otkin et al. 2016; Paimazumder and Done 2016; Wang et al. 2016; Yuan et al. 2018). Defining flash droughts is prudent not only in terms of their rates of intensification but also by what exactly constitutes a "drought" (Otkin et al. 2017). Our preliminarily accepted definition of flash drought was based on combinations of multiple hydroclimatic events using pentad intervals (Zhang et al. 2017a, 2018), but this definition only applies to short-term durations and does not really reflect the rapidity of drought events. The content of the present study is based on our previous work (Zhang et al. 2017a, 2018). Although it does not reflect flash drought events in a strict sense, the phenomenon described here falls into the category of concurrent drought and heatwave events. We used a combination of multiple hydroclimatic events based on pentad intervals to provide early warning information that may alert relevant personnel to prepare for the impact of a flash drought.

The Paris Agreement in December 2015 at the United Nations Framework Convention on Climate Change (UNFCCC) includes two long-term global temperature goals: "holding the increase in the global average temperature to well below 2.0 °C above pre-industrial levels and pursuing efforts to limit the temperature increase to 1.5 °C" (UNFCCC 2015). As opposed to the former 2.0 °C goal, limiting warming to 1.5 °C would significantly limit the effects of climate change (Schleussner et al. 2016). The 0.5 °C difference in global average temperature between these scenarios represents a large addition of energy into the global climate system which would carry enormous consequences (Hare et al. 2016).

At present, global temperature warming is about 1.0 °C above pre-industrial levels. This increase has severely impacted human livelihoods, social economies, and natural systems (Hare et al. 2016). If the world warms by 2.0 °C, many vulnerable countries and regions would be critically threatened. For example, a shift in global warming from 1.5 to 2.0 °C above pre-industrial levels would lead to great decrease of runoff, increase of long-term drought, and more occurring conditions for malaria transmission over drylands (Huang et al. 2017). For example, extreme events like the "2012–2013 Angry Summer" and the "Early 2016 Coral Sea Heat" of Australia would be likely to be reduced by at least 26 and 24% in a 1.5 °C-increase world relative to a 2.0 °C increase (King et al. 2017). Schleussner et al. (2017) observed dramatically high occurrence of temperature and precipitation extremes under an additional 0.5 °C warming. The glaciers in high mountains of Asia will be lost by $36 \pm 7\%$ under even 1.5 °C of warming by the end of the twenty-first century, as this area is consistently warming more rapidly than the global average (Kraaijenbrink et al. 2017).

The Coupled Model Intercomparison Project Phase 5 (CMIP5) has incorporated many comprehensive global climate models, which include not only historical simulations, but also future scenario simulations (Taylor et al. 2012). There are three future types of representative concentration pathway (RCP) scenarios commonly used in CMIP5 models (Meinshausen et al. 2011): the RCP2.6 (low forcing scenario), RCP4.5 (medium stabilization scenario), and RCP8.5 (high emissions scenario). Many researchers have applied CMIP5 to assess climate means and extremes in terms of historical or future periods (Knutti and Sedláček 2013; You et al. 2014; Jiang et al. 2015; Palazzi et al. 2015). Many researchers have assessed or projected individual occurrence of droughts and heatwaves using CMIP5 models (Nasrollahi et al. 2015; Russo et al. 2015; Venkataraman et al. 2016; Herrera-Estrada and Sheffield 2017), but concurrent drought and heatwave events have been relatively infrequently explored, especially short-term concurrent events.

Concurrent droughts and heatwaves pose greater potential socio-economic risks than individual occurrences, because the combination of these events can exacerbate their respective environmental and societal impacts. Even short periods of intense water deficit and heat stress can lead to significant agricultural yield loss if they occur within sensitive stages in crop development such as emergence, pollination, and grain filling (Kebede et al. 2012; Otkin et al. 2013). As a humid subtropical basin, the Gan River Basin has faced increasingly severe drought and heatwave stress in recent decades due to climate warming and stress upon available water resources (Tao et al. 2014; Zhang et al. 2015). Our previous work focused on short-term concurrent drought and heatwave characteristics based on meteorological observations and Variable Infiltration Capacity (VIC) simulations in the Gan River Basin (Zhang et al. 2017a), and on evaluation of the coupled model for short-term concurrent drought and heatwave simulations (Zhang et al. 2018). However, it is also important to quantify how short-term concurrent drought and heatwave risk changes under different future scenarios, especially at 1.5 versus 2.0 °C of global warming.

In humid subtropical regions, temperatures can easily reach high levels and lead to increase in evapotranspiration demand during growing/warming seasons. If precipitation deficits occur in the short-term, the positive feedback mechanism of high temperature and precipitation deficit readily results in short-term concurrent droughts and heatwaves. The differences between global warming levels of 1.5 and 2.0 °C are of special interest on short-term concurrent drought and heatwave events. To address these issues, we again used the Gan River Basin as a case study area and ran a set of ensemble simulations with the CMIP5-based VIC projections tailored specifically to 1.5 and 2.0 °C warming scenarios.

We used the downscaled CMIP5 outputs coupled with VIC model (CMIP5-VIC) in this study to project future changes in short-term concurrent droughts and heatwaves as the model can well capture regional hydro-climatological conditions (Zhang et al. 2018). We hope to provide a workable initial framework for the analysis of future short-term concurrent droughts and heatwaves in humid subtropical basins in a 1.5 and 2.0 °C world. The primary goals of this study were: (1) validation of the VIC performance in the soil moisture and evapotranspiration simulations; (2) verification of the two definitions of short-term concurrent droughts and heatwaves; (3) determination of years in which global warming would reach 1.5 or 2.0 °C thresholds under RCP4.5 or RCP8.5 scenarios; (4) projection of overall changes in short-term concurrent droughts and heatwaves in the Gan River Basin; and (5) projection of short-term concurrent droughts and heatwaves in the Gan River Basin at 1.5 versus 2.0 °C of global warming and assessment of differences in short-term concurrent droughts and heatwaves under an additional 0.5 °C of warming.

2 Materials and methods

2.1 Study area

The Gan River Basin is located within the central and southern parts of the Poyang Lake Basin, China (left panel of Fig. 1). Poyang Lake is the largest freshwater lake in China. The Waizhou hydrological station is located at the outlet of the Gan River Basin and controls 80,948 km^2 of the basin, at approximately the size of South Carolina in the U.S.; it receives about 678×10^8 m^3 of annual streamflow on average, representing the largest sub-basin both in area (51%) and runoff (50%) of the Poyang Lake Basin. The largest proportion of landform is mountainous areas and subordinate hills, mainly in the central and southern parts of the basin, while alluvial plains dominate the lower reaches of the basin. The Gan River Basin belongs to a subtropical humid monsoon climate zone and has average annual precipitation of 1600.1 mm and average annual temperature of 18.2 °C (Zhang et al. 2017a). The precipitation, soil moisture, evapotranspiration, and maximum temperature in Gan River Basin increase over the first half of the calendar year and decrease over the second half of the calendar year (Fig. 2). The annual average soil moisture, evapotranspiration, and maximum temperature of the basin were 244.7 mm, 687.8 mm, and 23.2 °C during 1961–2005. The runoff in this basin is mainly driven by precipitation and exhibits strong seasonality, again with an increase in the first half of the calendar year (typically reaching its peak in June) followed by a decline in the second half of the calendar year (typically reaching its lowest point in December).

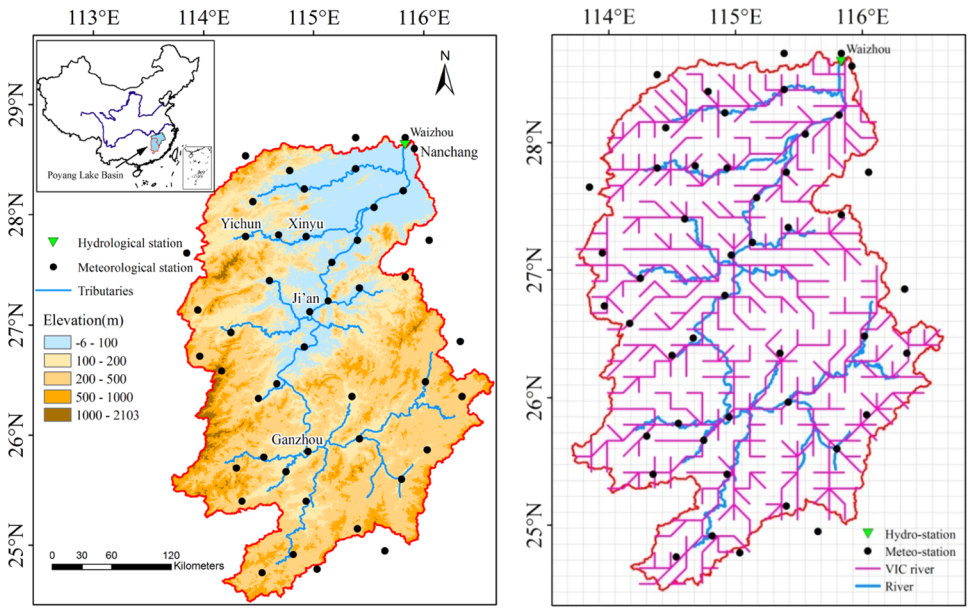

Fig. 1 Locations of 47 meteorological stations and hydrological station (outlet) in the Gan River Basin (left panel) and VIC river network to the basin outlet (right panel)

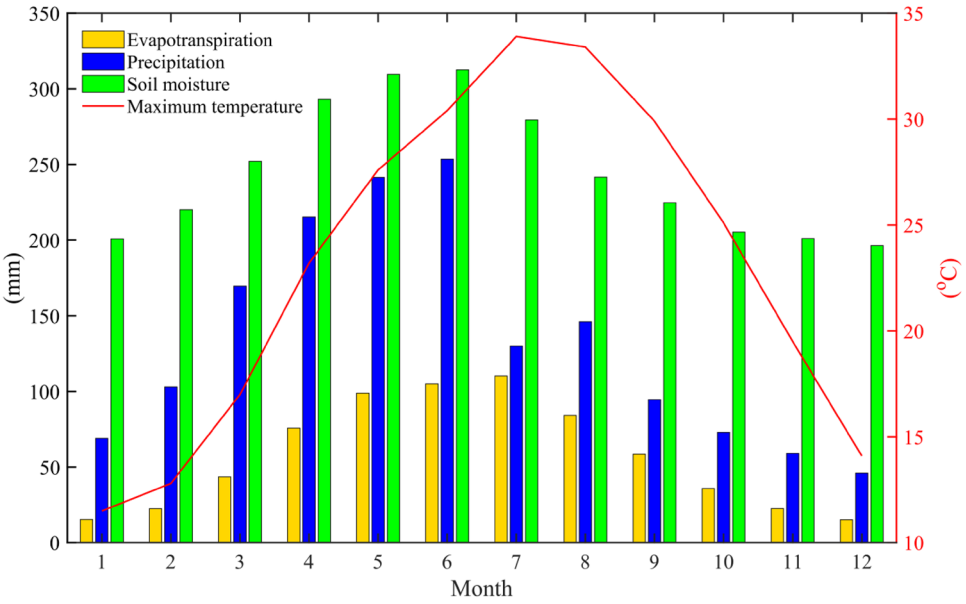

Fig. 2 Monthly mean evapotranspiration (mm), precipitation (mm), soil moisture (mm), and maximum temperature (°C) in the Gan River Basin from 1961 to 2005. Precipitation and maximum temperature are calculated based on 47 meteorological stations. Soil moisture and evapotranspiration are calculated based on the calibrated VIC model. Soil total column depth is about 1.5 m

2.2 Data

The outputs of average, maximum, and minimum temperature were obtained from 21 original CMIP5 models on the global scale (Taylor et al. 2012). We employed the historical period 1850–2005 and two RCP scenarios (RCP4.5 and RCP8.5) for the period 2006–2099 as most CMIP5 models include RCP4.5 and RCP8.5 scenarios. The names of these CMIP5 models are shown in Table 1. The global warming thresholds used in this study are relative to the pre-industrial levels (1850–1900), and serve to define the years in which global warming would reach 1.5 and 2.0 °C thresholds under RCP4.5 and RCP8.5 scenarios. We refer to well-established definitions of the 1.5 and 2.0 °C world (King et al. 2017). In order to obtain 1.5 and 2.0 °C stabilization targets, we calculated the global average surface temperature anomaly for the 30-year running mean based on a multi-model ensemble mean (21 original models). The 1.5 °C period (accurate

Table 1 CMIP5 models included in NEX-GDDP dataset

Model name	Modeling center (or group)	Model name	Modeling center (or group)
ACCESS1-0	Commonwealth Scientific and Industrial Research Organization (CSIRO)and Bureau of Meteorology (BOM), Australia	INMCM4	Institute for Numerical Mathematics, Russia
BCC-CSM 1-1	Beijing Cliamte Center, China Meteorological Administration, China	IPSL-CM5A-LR	Institut Pierre-Simon Laplace, France
BNU-ESM	College of Global Change and Earth System Science, Beijing Normal University, China	IPSL-CM5A-MR	
CanESM2	Canadian Centre for Climate Modelling and Analysis, Canada	MIROC5	The University of Tokyo, National Institute for Environmental Studies, and Japan Agency for Marine-Earth Science and Technology, Japan
CCSM4	National Center for Atmospheric Research, USA	MIROC-ESM-CHEM	
CESM1-BGC	Community Earth System Model Contributors, USA	MIROC-ESM	
CNRM-CM5	Centre National de Recherches Météorologiques/ Centre Européen de Recherche et Formation Avancée en Calcul Scientifique, France	MPI-ESM-LR	Max Planck Institute for Meteorology, Germany
CSIRO-MK3-6-0	Commonwealth Scientific and Industrial Research Organization/Queensland Climate Change Centre of Excellence, Australia	MPI-ESM-MR	
GFDL-CM3	Geophysical Fluid Dynamics Laboratory, USA	MRI-CGCM3	Meteorological Research Institute, Japan
GFDL-ESM2G		NorESM1-M	Norwegian Climate Centre, Norway
GFDL-ESM2M			

arrival year) is determined by the time when the 30-year running mean is between 1.3 and 1.7 °C (crossing the 1.5 °C threshold) warmer than the pre-industrial period. The 2.0 °C period is defined similarly. We utilized the ensemble mean of coupled models with two RCP scenarios to generate the 1.5 and 2.0 °C warmer worlds relative to the pre-industrial levels.

The NASA Earth Exchange Global Daily Downscaled Projections (NEX-GDDP) dataset (Thrasher et al. 2012) includes 21 downscaled CMIP5 outputs with daily precipitation, maximum temperature, and minimum temperature. This dataset was treated by the Bias-Correction Spatial Disaggregation method to downscale the projections from the 21 original CMIP5 models. Each of these downscaled outputs has a common horizontal resolution of 0.25° × 0.25°. This dataset used in this study includes a historical period from 1961 to 2005 and future period from 2006 to 2099 (RCP4.5 and RCP8.5). The detailed dataset information and documentation are available online (https://cds.nccs.nasa.gov/nex-gddp/).

To explore the changes in short-term concurrent droughts and heatwaves under 1.5 and 2.0 °C global warming levels, we used NEX-GDDP data as input data to run the calibrated VIC model and obtain evapotranspiration and soil moisture for each downscaled CMIP5-VIC. According to our previous research, the calibrated VIC (0.125° spatial resolution, right panel of Fig. 1) indeed reasonably simulates hydrological processes (Zhang et al. 2017a), and the downscaled CMIP5-VIC effectively captures the climatological characteristics of short-term concurrent droughts and heatwaves in the Gan River Basin (Zhang et al. 2018). The 21 available downscaled CMIP5 names are also listed in Table 1. We interpolated the downscaled CMIP5 outputs (0.25° × 0.25°) to a uniform grid with a 0.125° × 0.125° resolution for convenience in coupling the VIC model simulations.

2.3 Short-term concurrent drought and heatwave indices

We used pentad (5-day) means of the related hydro-meteorological variables to capture short-term concurrent drought and heatwave characteristics during crop growing seasons (March-October) in the Gan River Basin. There are two types of short-term concurrent droughts and heatwaves (described as "concurrent events" from here on) which are distinguishable by their core formation mechanisms. The first type is the heat wave concurrent event (HWCE), which is caused by persistent high temperatures that cause increase of evapotranspiration anomalies (energy-limited evapotranspiration) and subsequent rapid decreases in soil moisture. The second type is the precipitation deficit concurrent event (PDCE), which is triggered by persistent precipitation deficits that bring about the negative phase of soil moisture and evapotranspiration anomalies (water-limited evapotranspiration) and in turn cause temperature to rise.

According to the definitions provided by our previous study (Zhang et al. 2017a), an HWCE is identified when the specific requirements (maximum temperature anomaly > one standard deviation, evapotranspiration anomaly > 0, and soil moisture < 40th percentile) are satisfied for each grid and pentad. A PDCE occurs when conditions of maximum temperature anomaly > one standard deviation, evapotranspiration anomaly < 0, and precipitation < 40th percentile are met for each grid and pentad. A short-term concurrent drought and heatwave will occur when the definitions are met in each grid and each pentad. Each hydrometeorological variable anomaly is defined here as a departure from the climatology within crop growing seasons during the reference period (1961–2005).

The frequency of occurrence (FOC) is defined as the percentage of pentads under both types of concurrent events for each grid. For example, the FOCs of the specific grid for the future period (2006–2009) were calculated as the pentads of the concurrent events divided by the total number of pentads in this period and multiplied by 100%.

3 Results

3.1 VIC performance in soil moisture and evapotranspiration

The calibrated VIC streamflow simulations of our previous study were in accordance with streamflow observations (Zhang et al. 2017a). However, we did not perform any verification of soil moisture and evapotranspiration; the two datasets provide crucial information related to short-term concurrent droughts and heatwaves. In this study, we validated the VIC simulations (soil moisture and evapotranspiration) based on well-recognized data that is freely available online. The outputs from the VIC model used in this study are called VIC (Yuqing) data, with a total soil depth of around 1.5 m.

The first set of well-recognized data was derived from the Noah Land Surface Model, Version 3.3 (Rodell et al. 2004) in the Global Land Data Assimilation System, Version 2 (GLDAS v2). We used monthly soil moisture and evapotranspiration for this dataset with a spatial resolution of 0.25° (https://disc.sci.gsfc.nasa.gov/datasets/GLDAS_NOAH025_M_V2.0/summary?keywords=GLDA). We labeled this data as GLDAS v2 (Noah v3.3). It includes four soil layers: 0–0.1 m, 0.1–0.4 m, 0.4–1.0 m, and 1.0–2.0 m. The second dataset was obtained from the Land Surface Processes and Global Change Research Group (Institute of Geographic Sciences and Natural Resources Research, Chinese Academy of Sciences) (Zhang et al. 2014). This dataset was also

processed by VIC model including daily soil moisture and evapotranspiration with a spatial resolution of 0.25° (http://hydro.Igsnrr.ac.cn/public/vic_outputs.html). We labeled this data as VIC (Xuejun); the soil layer depth is similar to the VIC (Yuqing) data.

We used an anomaly method to compare the two sets of data at the same level (where different datasets include different total soil depths). As shown in Figs. 3 and 4, the monthly changes in soil moisture and evapotranspiration for VIC (Yuqing) and GLDAS v2 (Noah v3.3) were basically similar; their correlation coefficient (r) values exceed 0.8. The range of the VIC (Yuqing) box-and-whisker areas were larger than those of GLDAS v2 (Noah v3.3) and the standard deviation ratios were 1.2 and 1.3 for soil moisture and evapotranspiration anomalies, respectively, indicating that the amplitude of variations in VIC (Yuqing) was larger than those of GLDAS v2 (Noah v3.3). This may be due to the fact that more meteorological observations are assimilated by VIC (Yuqing) than GLDAS v2 (Noah v3.3). There are up to 47 meteorological stations in the Gan River Basin, which provided reliable meteorological input data for accurately simulating the hydrological processes.

According to Figs. 5 and 6, the VIC (Yuqing) simulations were in accordance with the VIC (Xuejun) model results at daily soil moisture and evapotranspiration anomalies. Their correlation coefficients (r) exceed 0.9. The lengths of the VIC (Yuqing) box-and-whisker areas were close to the VIC (Xuejun) as the standard deviation ratios were close to 1, indicating that their amplitude of variations were basically consistent. This further suggests that the VIC model we used very accurately simulates soil moisture and evapotranspiration in the Gan River Basin.

3.2 Validating the definition of concurrent events

The IPCC special report defines combinations of multiple climate extremes (compound events) in three approaches (IPCC 2012): (a) at least two extreme events occurring simultaneously or successively, (b) combinations of multiple extreme events with underlying conditions that amplify the impacts, and (c) combinations of multiple events that are not extremes at individual level but lead to an extreme event or impact when they combined. The short-term concurrent event definition of this study is similar to the definition under "(c)" in the IPCC special report.

We first investigated whether these concurrent events are characterized by heat waves under the two combinations of multiple hydroclimatic events (i.e., HWCE and PDCE events). Figure 7 shows the pentad mean of maximum temperature (T_{max}) under HWCE and PDCE events from 1961 to 2005. Under HWCE conditions, the pentad mean T_{max} reached 35.3 °C in the whole basin occupying 79.7% of total

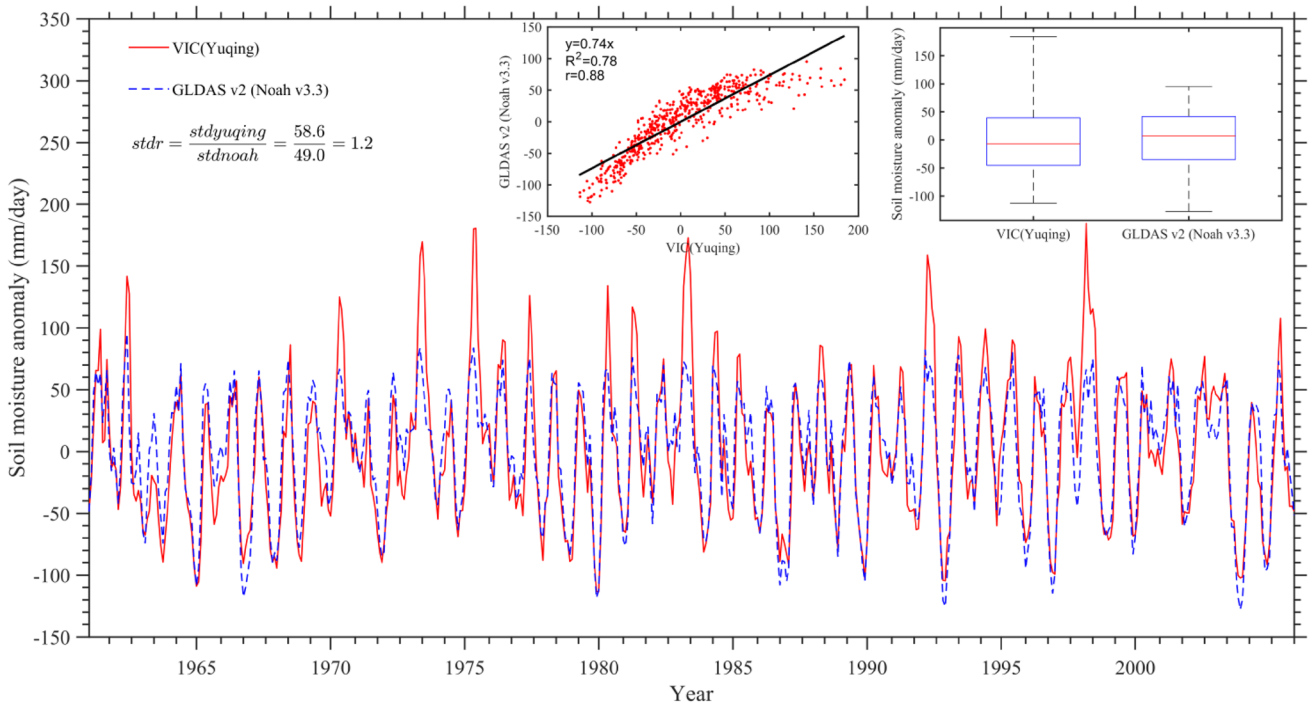

Fig. 3 Comparison between VIC (Yuqing) and GLDAS v2 (Noah v3.3) soil moisture anomalies at monthly timescales in Gan River Basin during 1961–2005. *stdr* standard deviation ratio of VIC (Yuqing) and GLDAS v2 (Noah v3.3) simulations in soil moisture anomalies. Correlation coefficient *r* is at $p < 0.05$ significance level. Top and bottom of the box (box-and-whisker plot) represent 75th and 25th percentiles; whisker indicates the range of soil moisture anomaly; red line denotes median value

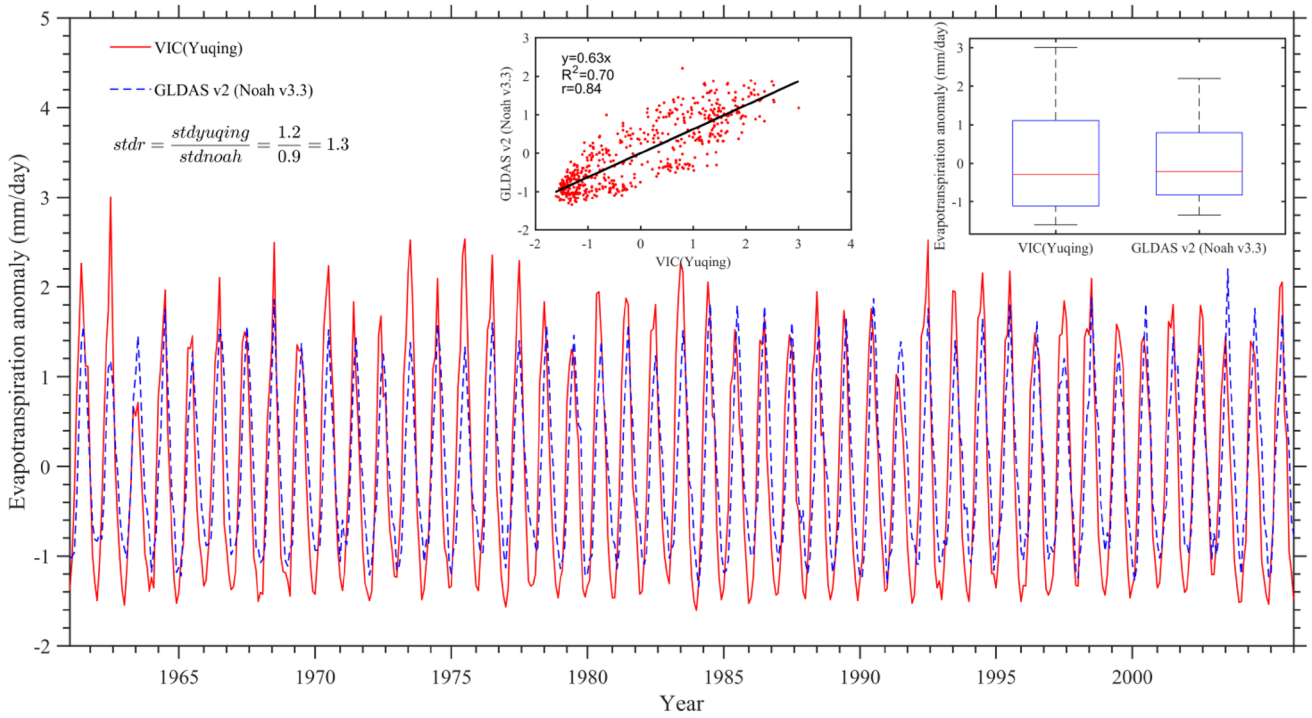

Fig. 4 The same as Fig. 3, but for evapotranspiration anomalies

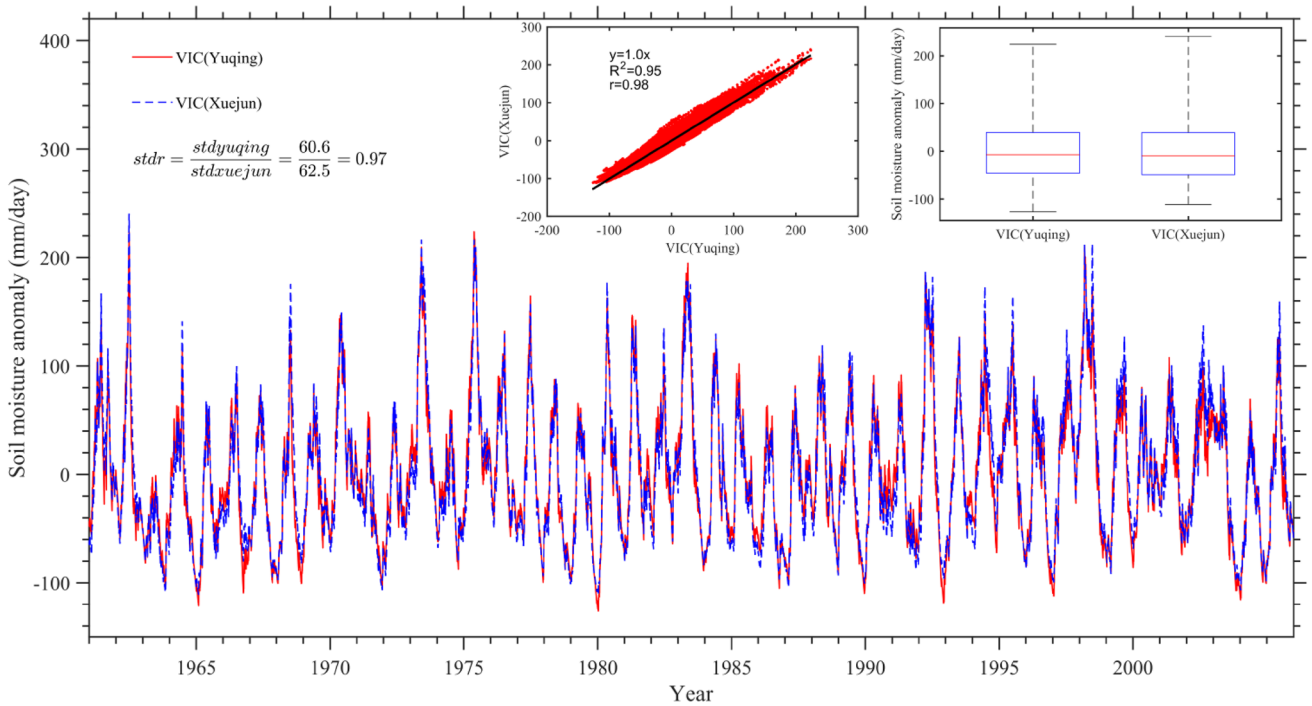

Fig. 5 Comparison between VIC (Yuqing) and VIC (Xuejun) soil moisture anomalies at daily timescales in Gan River Basin during 1961–2005. *stdr* standard deviation ratio of VIC (Yuqing) and VIC (Xuejun) simulations in soil moisture anomalies. Correlation coefficient r is at $p < 0.05$ significance level. Top and bottom of the box (box-and-whisker plot) represent 75th and 25th percentiles; whisker indicates the range of soil moisture anomaly; red line denotes median value

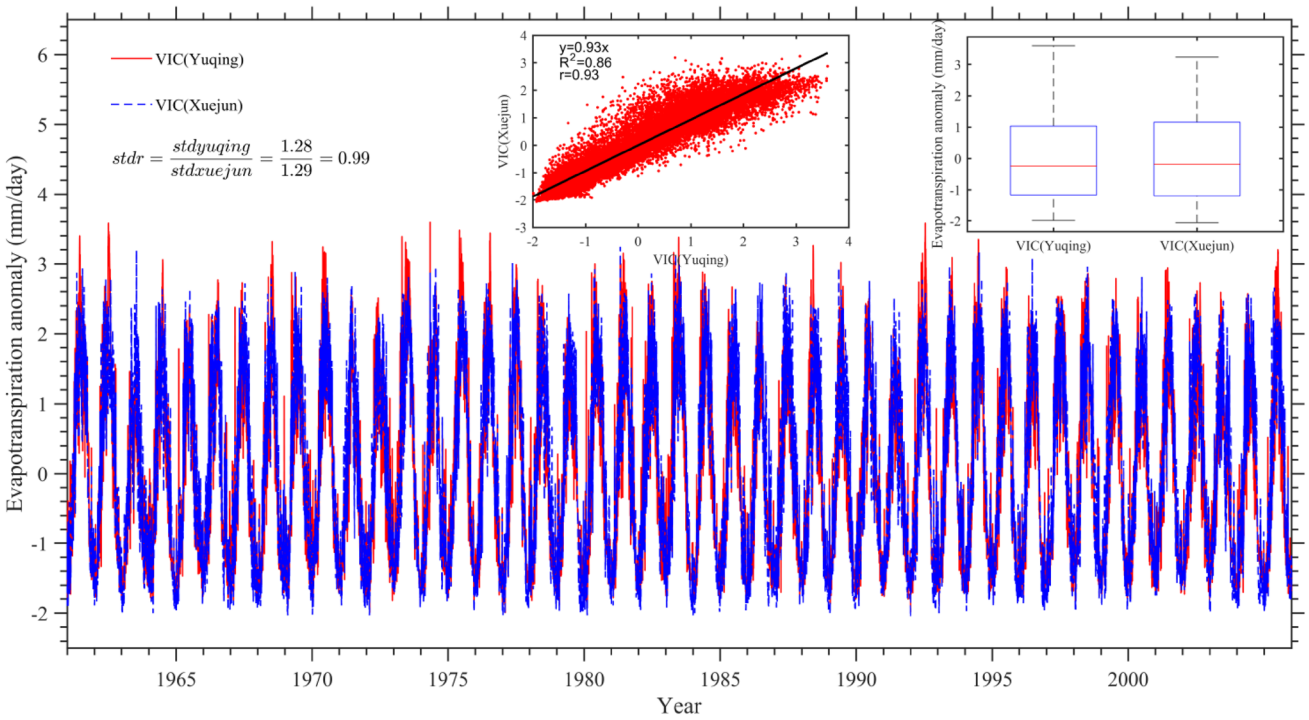

Fig. 6 The same as Fig. 5, but for evapotranspiration anomalies

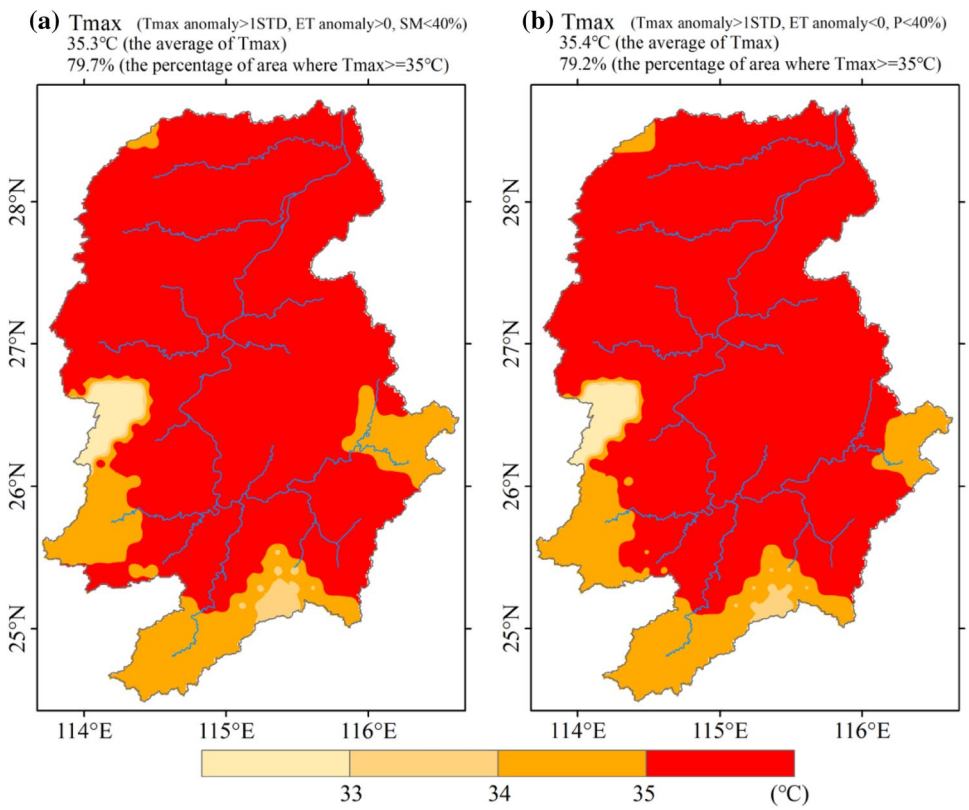

Fig. 7 Pentad mean of maximum temperature (T_{max}) under **a** heat wave concurrent events (HWCEs) and **b** precipitation deficit concurrent events (PDCEs) from 1961 to 2005

area where $T_{max} \geq 35$ °C (Fig. 7a). Under PDCE conditions, the pentad mean T_{max} reached 35.4 °C in the whole basin occupying 79.2% of total area where $T_{max} \geq 35$ °C (Fig. 7b). There are many definitions for heat waves. The World Meteorological Organization (WMO) recommends that a T_{max} greater than 32 °C for three consecutive days can be defined as a heat wave event, and the method proposed by China Meteorological Administration is similar to WMO, but with 35 °C as the threshold (You et al. 2017). Therefore, the T_{max} values under HWCE and PDCE are in accordance with the definitions of heat waves.

We next judged whether drought events under HWCE and PDCE conditions. The pentad drought status of climate division is assessed based on soil moisture percentiles consistent with the United States Drought Monitor (USDM): D0 drought (mild drought or abnormally dry) states that the condition falls below the 30th percentile, D1 drought (moderate drought) that the condition is less than the 20th percentile, D2 drought (severe drought) that the condition is less than the 10th percentile, D3 drought (extreme drought) that the condition is less than the 5th percentile, and D4 drought (exceptional drought) states that the condition is less than the 2nd percentile (Svoboda et al. 2002). Figure 8 shows the pentad mean of soil moisture percentile under HWCE and PDCE events from 1961 to 2005. Under HWCE conditions, the pentad mean soil moisture percentile of the basin is 27.7%, and the 83.9% of the total area in soil moisture percentile is less than 30% (Fig. 8a). The soil moisture condition under HWCE belongs to D0 drought. Under PDCE conditions, the pentad mean soil moisture percentile of the basin is 16.7%, and the 68.1% of the total area in soil moisture percentile is less than 20% (Fig. 8b). This soil moisture condition under PDCE belongs to D1 drought.

Therefore, HWCE and the PDCE can reasonably describe short-term concurrent drought and heatwave events.

3.3 Future timeframes for 1.5 and 2.0 °C global warming

We applied the 21 CMIP5 ensemble mean to project future changes in the global average surface temperature anomaly. As shown in Fig. 9, the global average surface temperature anomaly become stable at the end of the twenty-first century under the RCP4.5 scenario at about 2.6 °C higher than the pre-industrial level. The increase in temperature under RCP8.5 was faster than the increase under RCP4.5, with warming up to about 4.7 °C at the end of the twenty-first century.

Scenario RCP8.5 yields earlier 1.5 and 2.0 °C periods than RCP4.5, especially for the 2.0 °C scenarios (Fig. 9). The RCP4.5 scenario projects the 1.5 °C period from 2017 to 2036 (2027), which is a little later than the arrival time marked by RCP8.5 within 2016–2030 (2024) based on the 30-year running mean of the multi-model ensemble mean

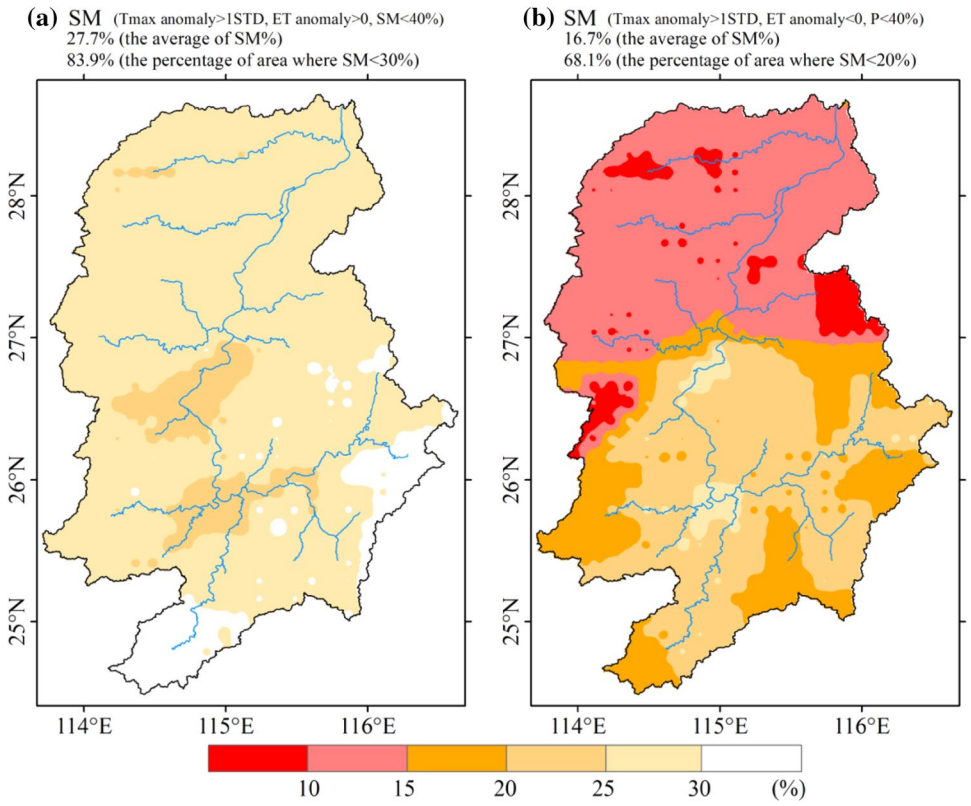

Fig. 8 Pentad mean of soil moisture (SM) percentile under **a** heat wave concurrent events (HWCEs) and **b** precipitation deficit concurrent events (PDCEs) from 1961 to 2005

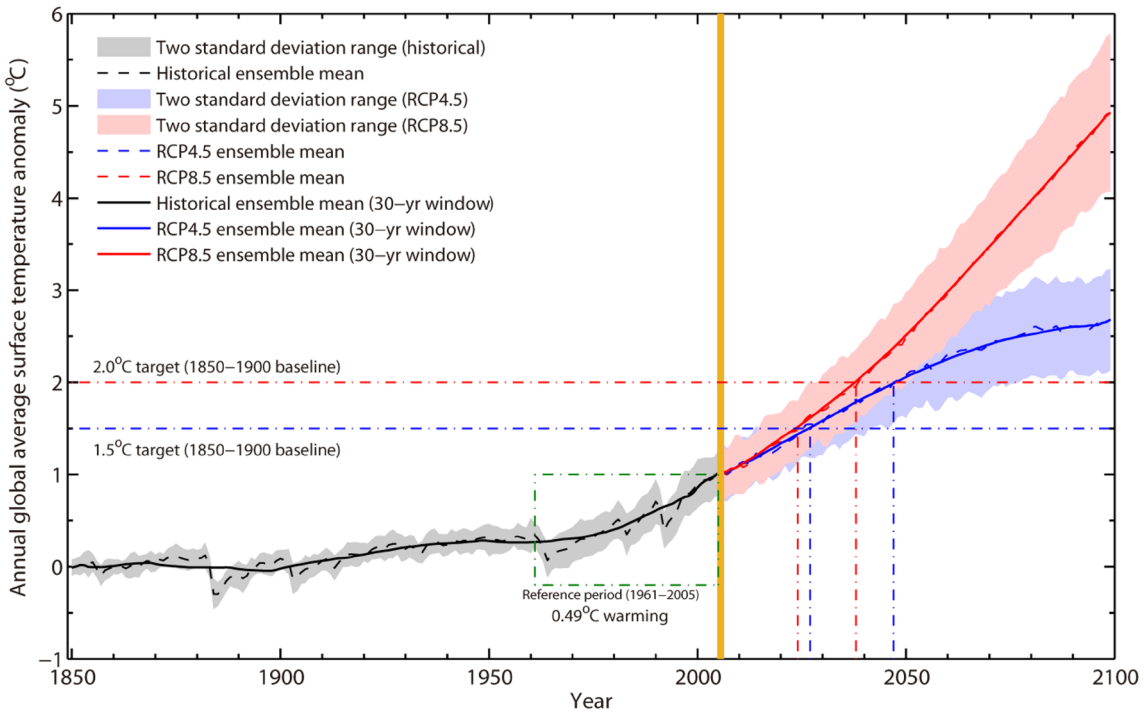

Fig. 9 Annual global average surface temperature anomaly based on multi-model ensemble simulation (baseline: 1850–1900)

Table 2 Years in which global average surface temperature relative to the pre-industrial levels (1850–1900) based on multi-model ensemble simulation (30-year running mean)

Scenario	1.5 °C (1.3–1.7 °C)	2.0 °C (1.8–2.2 °C)
RCP4.5	2027 (2017–2036)	2047 (2037–2059)
RCP8.5	2024 (2016–2030)	2038 (2031–2044)

(Table 2). Similarly, the RCP4.5 scenario projects the 2.0 °C period from 2037 to 2059 (2047), nearly 10 years later than RCP8.5, which projects it from 2031 to 2044 (2038). The faster warming rate under RCP8.5 marked faster crossing of both 1.5 and 2.0 °C thresholds. Both 1.5 and 2.0 °C periods also had relatively narrower timeframes under RCP8.5 than RCP4.5.

As shown in Table 3, the temperature changes over both China and the Gan River Basin are similar in RCP4.5 and RCP8.5 scenarios when the same global warming threshold is reached. The average temperature changes over China reach 1.81 °C in RCP4.5 and 1.82 °C in RCP8.5 under the 1.5 °C global warming level. The China-level warming exceeds the global levels, especially for minimum temperature, with a 2.03 °C increase with 1.5 °C of global warming and 2.77 °C increase with 2.0 °C of global warming. The average temperature reaches 1.82 °C when the global warming reaches 1.5 °C, suggesting that China will warm 0.32 °C above the global level. Similarly, when the global warming reaches 2.0 °C, the corresponding average temperature in China is 2.56 °C; in other words, China will see 0.56 °C more warming than the world level at this threshold. The level of warming over the Gan River Basin is close to the

Table 3 Changes in average temperature (T_{ave}), maximum temperature (T_{max}), and minimum temperature (T_{min}) under 1.5 °C and 2.0 °C global warming, respectively

Region	Scenario variable	1.5 °C			2.0 °C			2.0−1.5 °C
		RCP4.5	RCP8.5	AVE	RCP4.5	RCP8.5	AVE	AVE
China	T_{ave}	1.81	1.82	1.82	2.60	2.52	2.56	0.75
	T_{max}	1.64	1.65	1.65	2.44	2.36	2.40	0.76
	T_{min}	2.01	2.04	2.03	2.80	2.73	2.77	0.74
Gan River Basin	T_{ave}	1.41	1.39	1.40	2.09	1.95	2.02	0.62
	T_{max}	1.36	1.34	1.35	2.06	1.96	2.01	0.66
	T_{min}	1.46	1.47	1.47	2.12	1.97	2.05	0.58

Unit is °C

global warming level, however, because the basin is located in a low latitude and humid monsoon climate zone. The humid environment absorbs more radiant energy, thereby suppressing temperature increases similar to the mechanisms of endothermic oceans (Kintisch 2014).

3.4 Future changes in short-term concurrent droughts and heatwaves

We selected 1961–2005 as the reference period for investigating future changes in short-term concurrent droughts and heatwaves in the Gan River basin. HWCE events appear to increase in the future to slightly greater degree in the RCP8.5 than the RCP4.5 scenario (Fig. 10). The median values of RCP8.5 increased at a rate of 0.19 pentads/decade from 2006 to 2099 but only 0.08 pentads/decade in the RCP4.5. The amplitude medians of future HWCE pentads were greater than the reference period due to their standard deviation ratio greater than 1 (Fig. 10 shows that $std1 = 2.1$ and $std2 = 1.6$ of the future HWCE), indicating that the degrees of median instability grow increasingly severe as the temperature rises, especially for RCP8.5. The 25th -75th range amplitude of RCP8.5 is higher than that of RCP4.5, indicating relatively large uncertainties of the HWCE in the high emissions scenarios.

As shown in Fig. 11, the PDCE medians presented a significant ($p < 0.05$) increase from 2006 to 2099, especially for the RCP8.5 scenario with a linear rate of 0.4 pentads/decade. The amplitude medians of future PDCE pentads ($std1 = 2.5$ and $std2 = 1.8$ for the future PDCE) are greater than those of the HWCE ($std1 = 2.1$ and $std2 = 1.6$ for the future HWCE), indicating that the PDCE pentads are less stable than those of HWCE with increasing temperature. The future 25th -75th range for PDCEs is larger than the reference period, implying greater uncertainty.

We next assessed future changes in the number of pentads for short-term concurrent events averaged over the Gan River Basin based on multi-model ensemble simulations at 25th, 50th (median), and 75th percentiles, respectively (Fig. 12). All of these values substantially increased in the future for both types of concurrent events, though the overall increase in PDCEs was higher than the increase in HWCEs and higher under the RCP8.5 than the RCP4.5 scenarios. The most substantial increase was observed in 25th percentile values, followed by 50th and 75th percentiles.

How do the prevalence and severity of the concurrent events change as the global temperature increases under the RCP4.5 versus the RCP8.5 scenarios? In order to straightforwardly assess these changes, we applied a 30-year moving average to eliminate any large annual fluctuations in

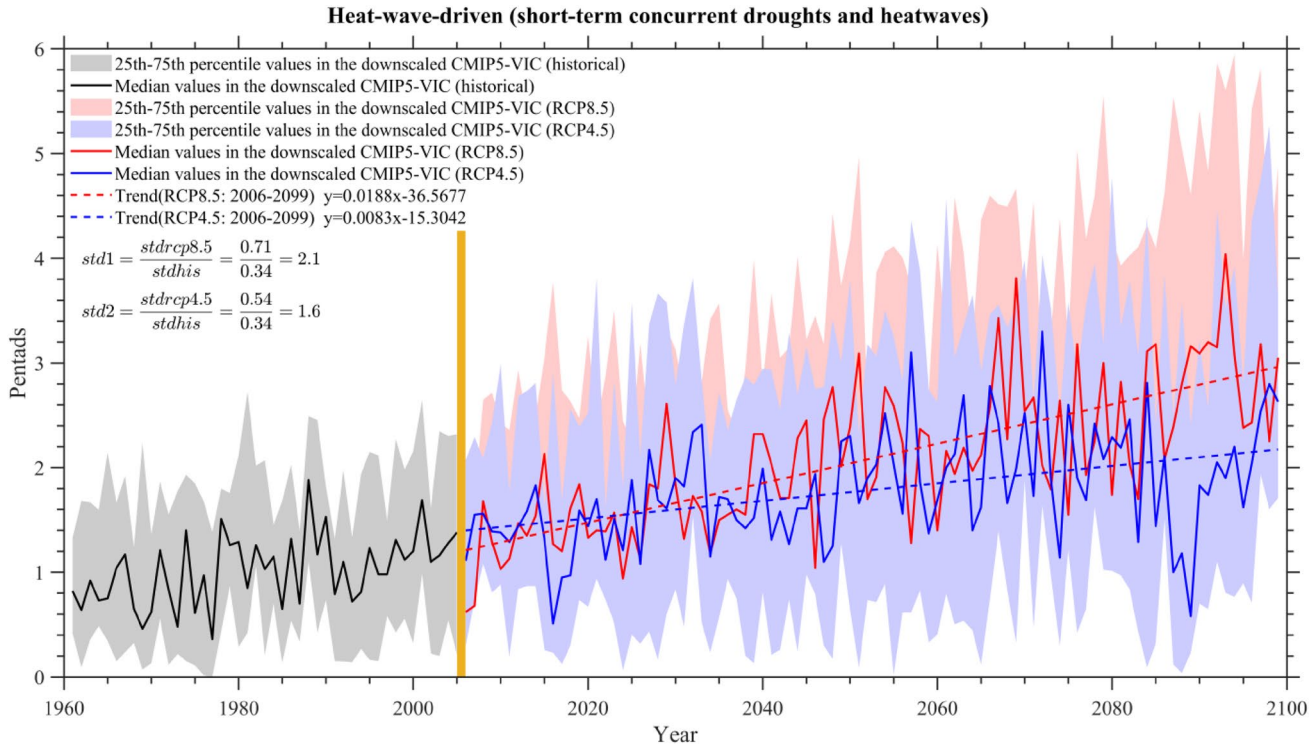

Fig. 10 Number of pentads under HWCE per year averaged over the Gan River Basin based on multi-model ensemble simulation (reference period: 1961–2005). Linear trends are at $P < 0.05$ significance level. *std1* standard deviation ratio of RCP8.5 and historical simulations in median values of multi-model ensemble results; *std2* is similar to *std1*, but for RCP4.5

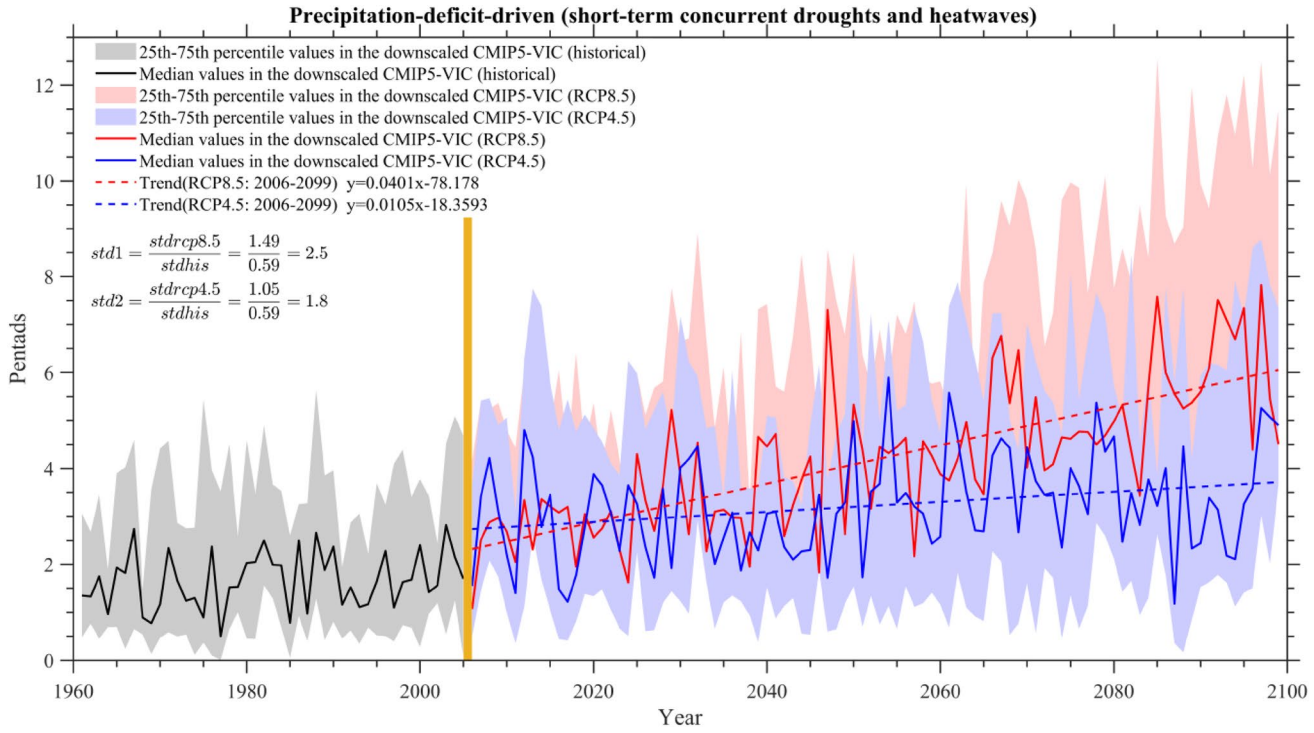

Fig. 11 As in Fig. 10, but for PDCE

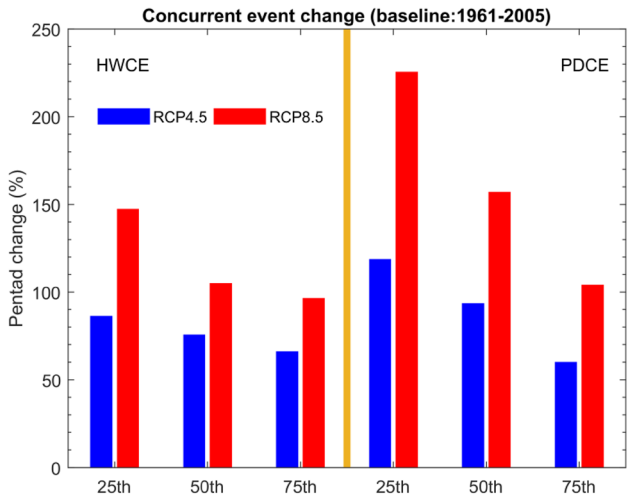

Fig. 12 Future climatological (2006–2099) changes in number of pentads for HWCE and PDCE events averaged over the Gan River Basin based on multi-model ensemble simulation at 25th, 50th (median), and 75th percentile values, respectively. Reference period: 1961–2005

concurrent events. As shown in Fig. 13, we found that the increase rate for HWCEs is higher in the RCP8.5 than the RCP4.5 scenario. Under RCP4.5 scenario, HWCE pentad changes increased from 17 to 74% in median values or from 32 to 90% in average values at the global warming from 1.1 to 2.4 °C. Under RCP8.5, the pentad changes of HWCE increased by 37%-150% for median values and 26%-178% for average values from the global warming 1.1 to 4.5 °C, respectively. The pentad changes of PDCE are similar to those of HWCE. Under RCP4.5 and 8.5 scenarios, the pentad changes of PDCE are projected to increase by 44–77% (56–80%) in the median values (average values) from the global warming 1.1 to 2.4 °C, and by 48–171% (42–197%) in the median values (average values) from the global warming 1.1 to 4.5 °C, respectively. As the global temperature increased, we observed a larger 25th–75th range in both types of concurrent events and especially under RCP8.5. In general, both types of concurrent events appear to linearly increase with global warming in Gan River Basin.

A large multi-model ensemble can reduce the uncertainty caused by inter-model variability and effectively represent the climatology of a given region. We applied the multi-model ensemble mean to investigate the spatial FOC patterns of concurrent events. We calculated the future FOCs of the concurrent events in terms of spatial patterns, and found that future global warming is likely to increase the likelihood of concurrent events (Fig. 14). According to Fig. 14a, the future (2006–2099) HWCE FOCs in southernmost areas of the basin will markedly increase (greater than 200%) with respect to the reference period, and decrease from south to north (below 60% in the northeastern parts of the basin). The future increases in PDCE FOCs are mainly distributed

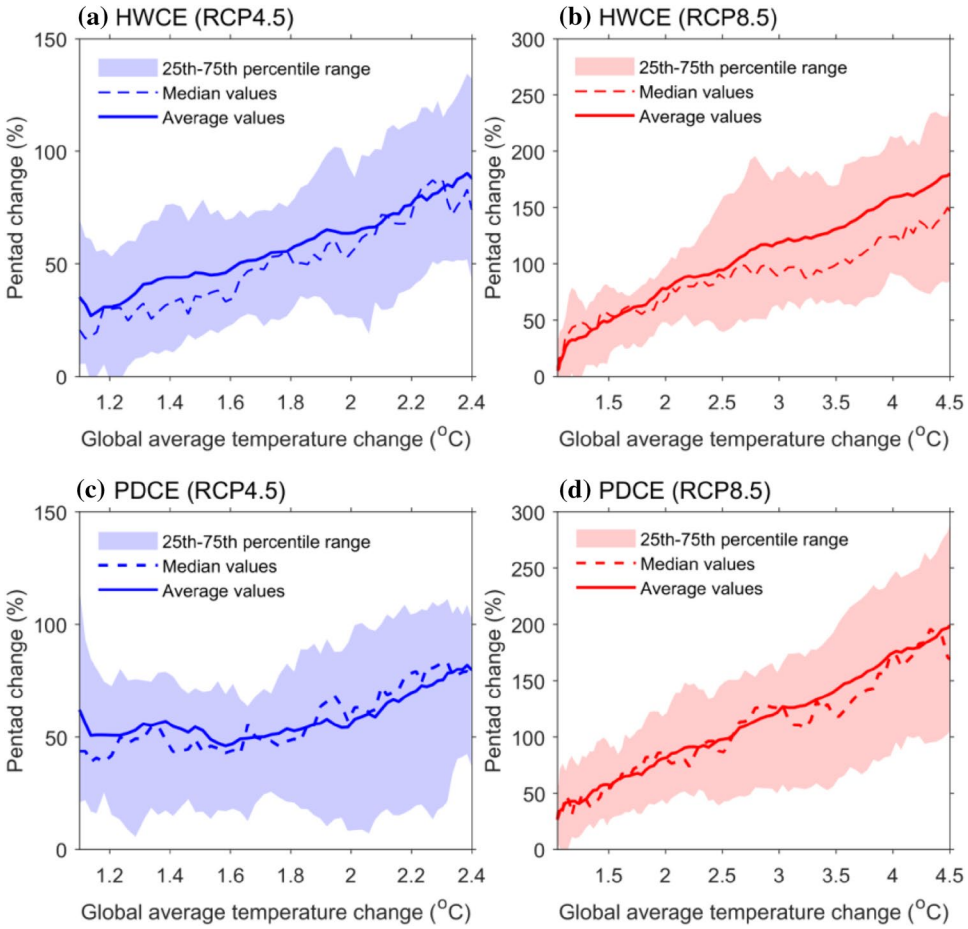

Fig. 13 Changes in number of pentads for HWCE and PDCE events under RCP4.5 and RCP8.5 scenarios per year averaged over the Gan River Basin. Multi-model ensemble mean is calculated with a 30-year running mean to eliminate the strong fluctuation of time series in the pentads of concurrent events. Reference period: 1961–2005

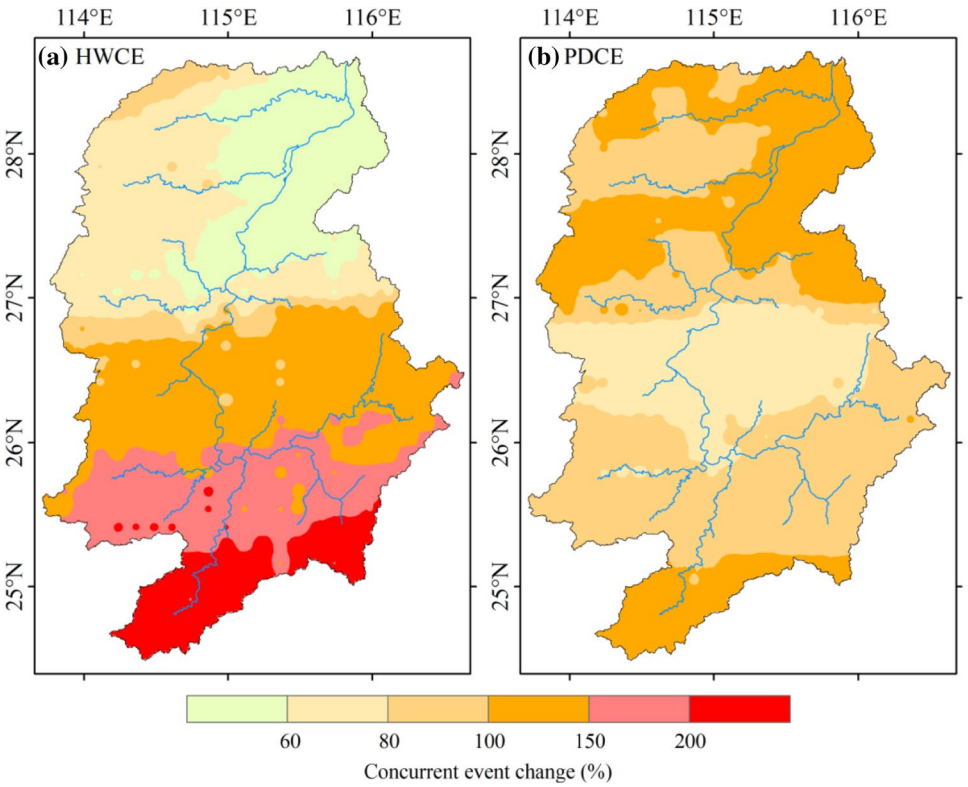

Fig. 14 Changes (future period minus reference period) in FOCs for **a** HWCEs and **b** PDCEs. Future scenario (2006–2099) is average of RCP4.5 and RCP8.5 scenarios. Reference period: 1961–2005

between 60 and 150% (Fig. 14b), and depart from the corresponding HWCE FOC distribution. There are relatively small increases in PDCE FOCs in central parts of the basin, and rising trend towards the northern and southern parts of the basin.

The FOC of concurrent event distributions discussed above may be directly related to the historical distributions (Zhang et al. 2017a), so we next sought the role of global warming in these increases. As shown in Fig. 15, a clear inverse relationship exists between the historical FOC and future FOC changes of concurrent events in the Gan River Basin, indicating that a region with fewer concurrent events (<1.5 pentads in HWCE and <3.0 pentads in PDCE) in the historical period would experience a multi-fold increase ($>100\%$) in the future while high-frequency areas (>4 pentads in HWCE and >6 pentads in PDCE) would experience a substantial increase (around 50–80%) in the future. This phenomenon is more obvious in HWCEs (Fig. 15a), with nearly exponential distribution in the changes of FOCs.

3.5 Changes in concurrent events with 1.5 and 2.0 °C global warming

We calculated the spatial FOC changes of concurrent events at global warming of 1.5 and 2.0 °C based on RCP4.5 and RCP8.5 scenarios (Fig. 16). The overall FOC increments for HWCEs decreased from south to north in both 1.5 and 2.0 °C worlds. These FOCs are projected to increase by more than 30% over the most of the basin under 1.5 °C global warming (Fig. 16a), but a further increase to 2.0 °C intensifies the FOC increase to 50% over the most of the basin (Fig. 16b). If the projected warming decreases from 2.0 to 1.5 °C, the FOC increments for HWCEs are reduced by as much as 50% with the largest reductions in the southernmost areas of the basin (Fig. 16c). PDCE FOCs clearly show a gradient distribution pattern. These FOCs are projected to increase by 50–70% over the most of the basin under a 1.5 °C world (Fig. 16d). There are about 50–90% increases in PDCE FOCs in most of the basin with 2.0 °C of global warming (Fig. 16e), with about half of the basin experiencing increases above 70%. If the projected warming value decreases from 2.0 to 1.5 °C, the increments of FOC for PDCEs are reduced by about 10–20% across most of the basin (Fig. 16f).

In summary, warming by either 1.5 or 2.0 °C appears to result in an increase in both HWCE and PDCE events by more than 50% in most of the Gan River Basin relative to the reference period. An additional 0.5 °C of warming from 1.5 to 2.0 °C causes most of the basin to experience around an increase in 20% with the occurrence of concurrent events.

We also found an obvious negative relationship between the historical FOCs of concurrent events and the increased FOC of concurrent events at 1.5 or 2.0 °C of global warming in terms of spatial patterns across the basin (Fig. 17). The correlation coefficients of HWCE FOCs between their historical values and future increments at 1.5 or 2.0 °C are around -0.80, and about -0.60 for PDCEs, indicating that the negative correlation is more obvious for HWCEs than PDCEs. We observed substantial increases ($>80\%$ in HWCE and $>50\%$ in PDCE) in low-value areas (<1.5

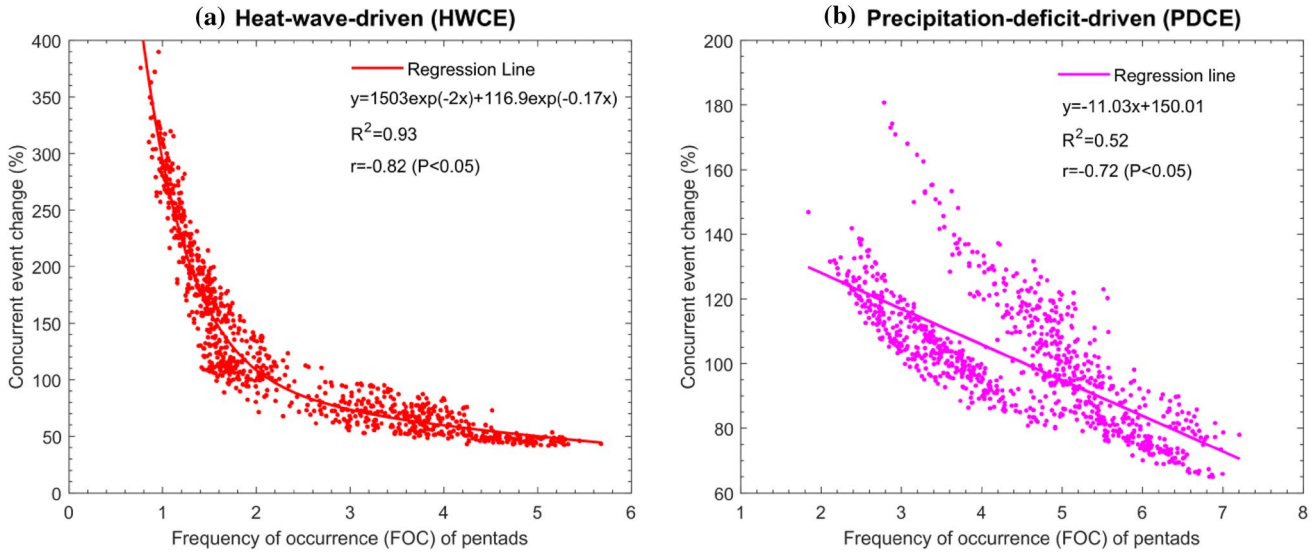

Fig. 15 Scatter plot of Gan River Basin FOCs for **a** HWCEs and **b** PDCEs against future changes relative to the reference period. X-axis represents historical FOCs and y-axis denotes changes in future FOCs. Future scenario is the average of RCP4.5 and RCP8.5 scenarios. Reference (historical) period: 1961–2005. Regression line is applied by total least square. *r* is correlation coefficient exceeding 0.05 significance level

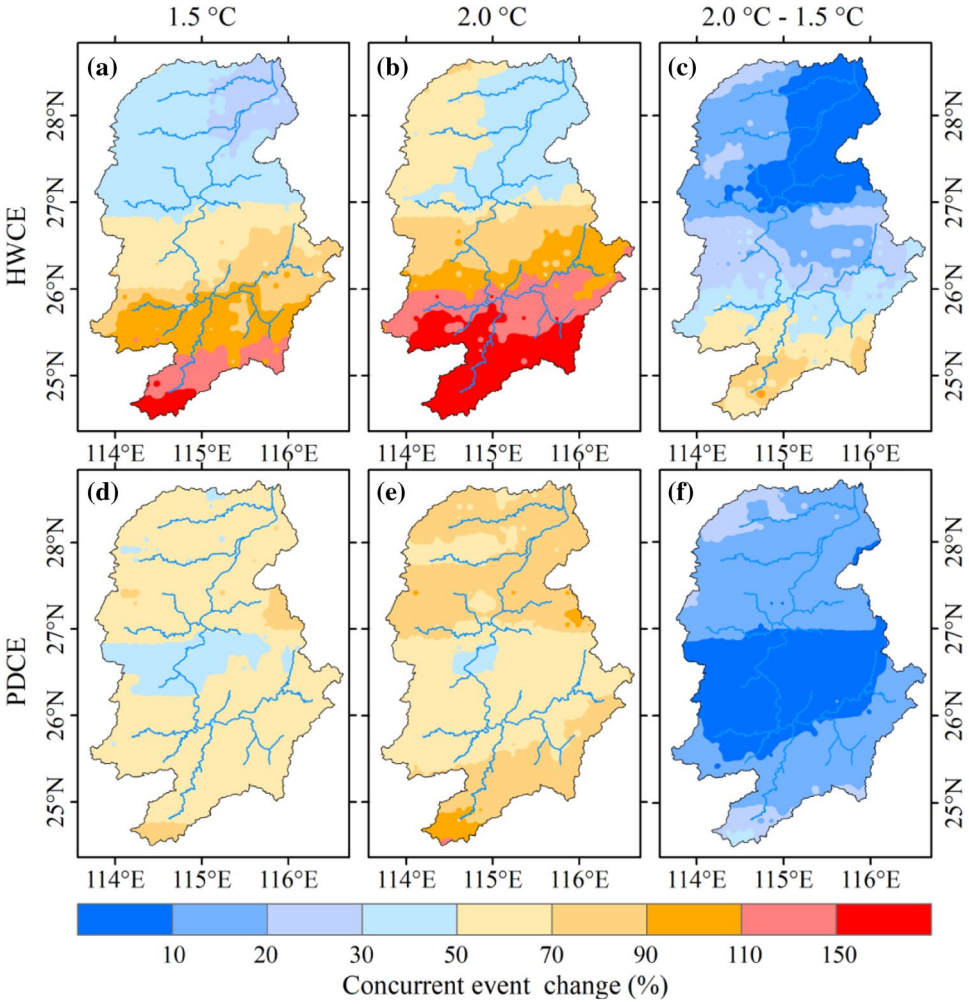

Fig. 16 Changes (future period minus reference period) in FOCs of HWCE and PDCE events under 1.5 and 2.0 °C warming with additional 0.5 °C warming. The changes of concurrent events in the 1.5 °C (or 2.0 °C) scenario are the average changes of the 1.5 °C (or 2.0 °C) warming period under the RCP4.5 and RCP8.5 scenarios. Reference period: 1961–2005

pentads in HWCE and < 3.0 pentads in PDCE) corresponding to both types of concurrent events in a 1.5 or 2.0 °C world, but especially for HWCEs. If the projected warming decreases from 2.0 to 1.5 °C, the HWCE FOC increments are reduced by at least 30% across the low historical FOCs (< 1.5 pentads) of the basin while the PDCE FOC increments are reduced by about 15% across most of the basin.

We also quantified cumulative density functions (CDFs) for the spatial FOCs of the concurrent events between the 1.5 and 2.0 °C warming scenarios. As shown in Fig. 18, we found substantial changes in these values between the reference period and future projections. Concurrent events intensify throughout the basin in 1.5 and 2.0 °C worlds compared to the historical FOCs, as marked by the movement towards the right side of the CDF curves. The curves under 2.0 °C warming shift farther towards the right than those under 1.5 °C, indicating greater frequency of both types of concurrent events in a 2.0 °C world. Such an increase in the concurrent events in the Gan River Basin could be interpreted as a "new normal".

We further assessed climatological changes in the number of pentads for the concurrent events at 1.5 and 2.0 °C of global warming over the Gan River Basin based on multi-model ensemble simulation at 25th, 50th (median), and 75th percentile values, respectively (Fig. 19). Under RCP4.5 scenario, increases in HWCEs are close to each other across all three percentiles. However, the 25th percentile increase in PDCEs is much higher than the other two (Fig. 19a). Under the RCP8.5 scenario, the largest increases in both types of concurrent events originate in the 25th percentile values (Fig. 19b). Overall, the percentile increases of RCP8.5 scenario are about 10–20% higher than those of the RCP4.5 scenario.

We next calculated the average increases in concurrent events between RCP4.5 and RCP8.5 scenarios in both 1.5 and 2.0 °C worlds. As shown in Fig. 19c, both 1.5 and 2.0 °C warming correspond to maximum increase by greater than 60% in HWCEs and higher than 90% in PDCEs in the 25th percentile values, respectively. Generally, increases are more obvious in all three percentiles for PDCEs than in HWCEs and to greater extent in a 2.0 °C world than a 1.5 °C

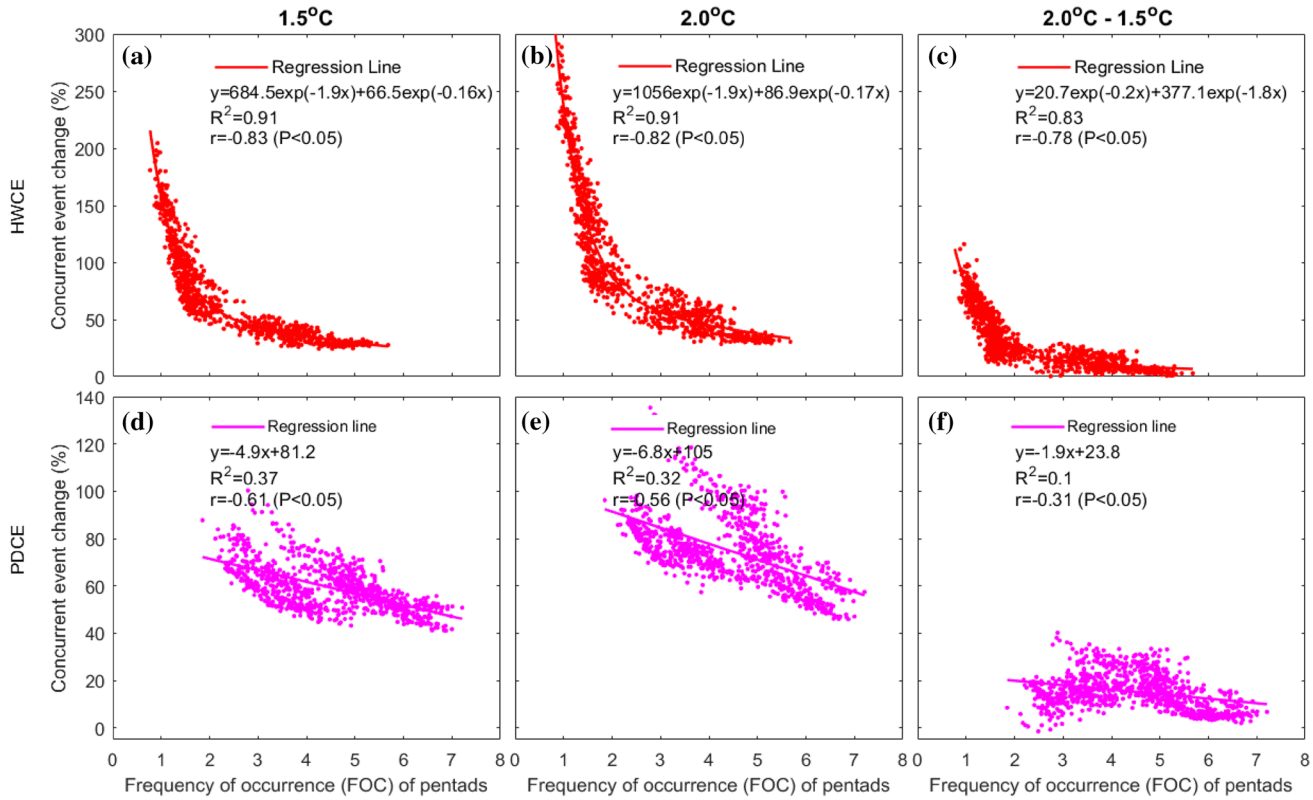

Fig. 17 Scatter plot of Gan River Basin FOCs for **a** HWCEs and **b** PDCEs against different future scenarios (1.5, 2.0 °C, and additional 0.5 °C warming) relative to the reference period 1961–2005. X-axis represents historical FOCs and y-axis denotes changes in future FOCs. Regression line is applied by total least square. *r* is the correlation coefficient exceeding the 0.05 significance level

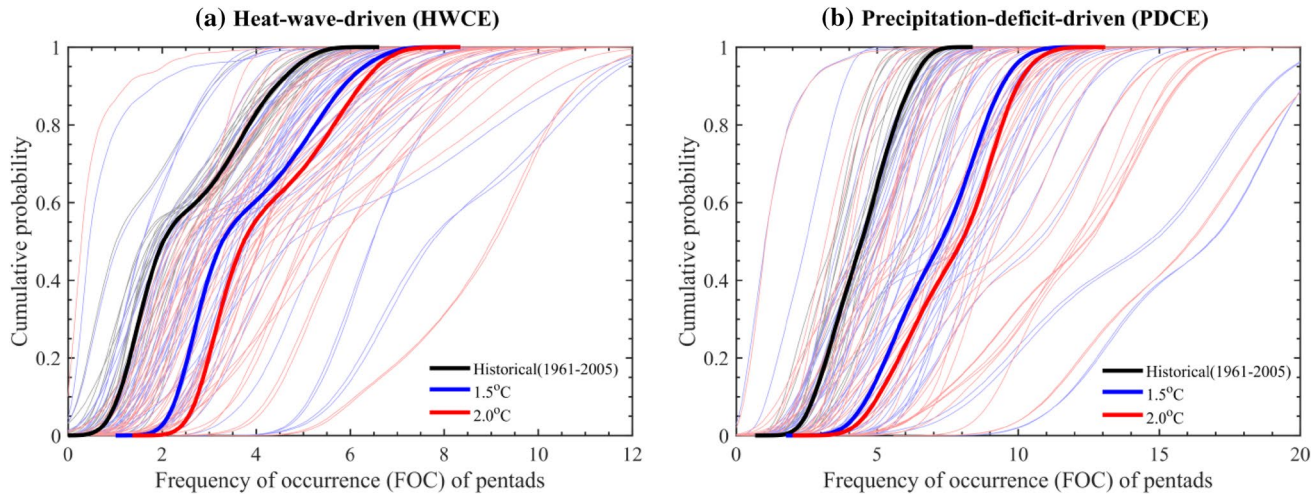

Fig. 18 Cumulative density functions of FOCs for **a** HWCEs and **b** PDCEs under different future scenarios (historical, 1.5 °C, and 2.0 °C). Thick black line represents historical multi-model ensemble mean, thin black line represents simulation for each model (21). Thick blue line represents 1.5 °C scenario multi-model ensemble mean, thin blue line represents simulation for each model (21 × 2) under RCP4.5 and RCP8.5 scenarios. Thick and thin red lines correspond to thick and thin blue lines

world. The differences between impacts at 1.5 and 2.0 °C of global warming levels are shown in Fig. 19d. Increases in HWCEs under an additional 0.5 °C warming are about 17%; differences between 25th, 50th, and 75th percentile values are very close. There is less dramatic increase in PDCEs under an additional 0.5 °C than HWCEs. If warming is

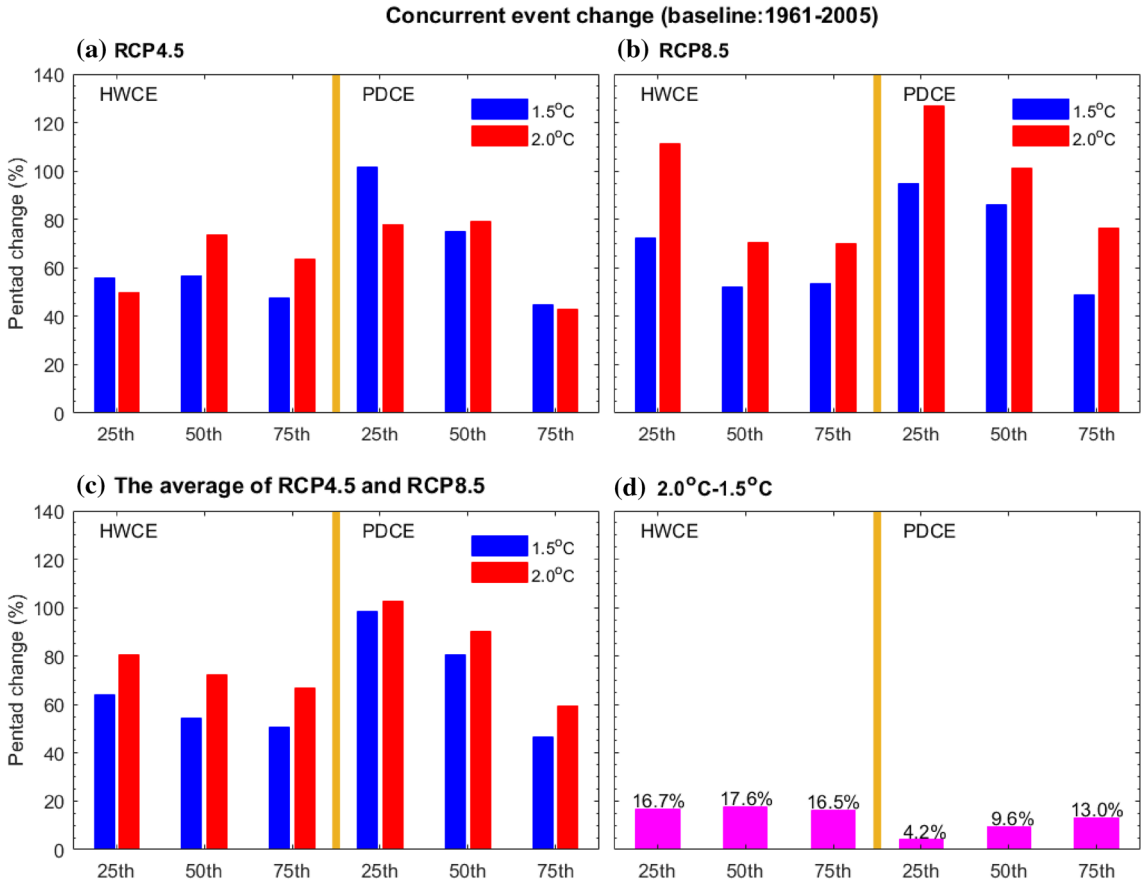

Fig. 19 Number of pentads for HWCE and PDCE changes at 1.5 and 2.0 °C warming levels with respect to reference period (1961–2005) per year averaged over the Gan River Basin based on multi-model ensemble simulation at 25th, 50th (median), and 75th percentile values, respectively

reduced from 2.0 to 1.5 °C, the frequency and intensity of the concurrent events are reduced by 9.6–17.6% in terms of climatological median pentads.

4 Discussion

We applied an ensemble mean of 21 CMIP5 models to discover that the global average surface temperature anomaly reaches about 2.6 and 4.7 °C above pre-industrial levels at the end of the twenty-first century under RCP4.5 and RCP8.5 scenarios. We also found that 1.5 °C of global warming may be reached by the year 2027 according to RCP4.5, while RCP8.5 pushes this threshold (1.5 °C) to the year 2024. Both RCP scenarios suggest that a 2.0 °C global increase will arrive in the middle of the twenty-first century. To this effect, the current RCP scenario design (including the lowest scenario, RCP2.6) is not ideal for ambitious mitigation for carbon dioxide (Mitchell et al. 2016). There is urgent demand for new climate change data-sets such as the half-a-degree additional warming projections, prognosis, and impacts (HAPPI) experiments (Mitchell et al. 2017) and the CMIP6 (Meinshausen et al. 2017).

The HWCE pentad medians slightly increase over the reference period, but there is no corresponding trend in PDCE events. The CMIP5 models were able to reproduce the effects of warming during the reference period (Chen and Frauenfeld 2014); this warming rate was also added to HWCE simulations because of the temperature-driven nature of this type of concurrent event. Precipitation in this region presents interannual fluctuations with no obvious upward or downward trends across the reference period (Zhang et al. 2017b). The CMIP5 can also reasonably capture the interannual variation characteristics of precipitation, so these characteristics were added to the PDCE simulations. The RCP4.5 and RCP8.5 scenarios show varying extent of warming effects due to radiation forcing (Meinshausen et al. 2011), which strengthen the precipitation fluctuations and temperature increases to form an overall projected increase in future concurrent events.

In general, similar to other climate extremes (Wang et al. 2017), there is a substantial increase in the climatological

pentads of the concurrent events in the Gan River Basin with the global warming. However, we observed future substantial increase in historical low-value areas greater than in historical high-value regions in the spatial FOCs of the concurrent events in the basin. Non-linear growth in climate events may occur at global or regional scales under different global warming thresholds (Knutti et al. 2015; Good et al. 2016; Schleussner et al. 2016), which produced non-linear FOC increases in different parts of the basin in response to the same global warming levels in this study. Concurrent droughts and heatwaves caused by higher warming levels represent non-linear increase, which threat agricultural products, social economies, and human health.

Northeastern China experienced increasingly frequent concurrent droughts and heatwaves, with second position only to southern China during 1979–2010 (Wang et al. 2016); the average temperature rate in northeastern China is about 0.5 °C higher than that in southern China. We infer that the increase in the concurrent event occurrence rate in northeastern China (medium and high latitude semi-humid areas) is much higher than that in southern China (medium and low latitude humid areas). The difference between them is also larger than that of the Gan River basin under global warming of 1.5 °C and 2.0 °C.

Even if the CDF of the multi-model ensemble mean moves rightward in the graph shown in Fig. 18, there are obvious differences in future concurrent event projections between the models we used here under the same warming threshold. These differences create large uncertainties in the future concurrent event predictions. The uncertainty range is generally not only affected by original CMIP5 models (Taylor et al. 2012), but also by various downscaling methods (Woznicki et al. 2016). In the RCP scenario, a greater temperature increase corresponds to a wider uncertainty range (Meinshausen et al. 2011). The performance of global climate models coupled with hydrological models can be improved via downscaling approaches deployed to simulate regional hydroclimatology variables (Sharma and Babel 2013; Zhang et al. 2016). Although the downscaled CMIP5 outputs from NEX-GDDP dataset are well-recognized (Thrasher et al. 2012), even minor errors in spatial downscaling among single variables of this dataset can enlarge errors in concurrent event simulations because a concurrent event is defined by the combination of multiple variables. Concurrent events are related to high temperatures, so the findings of this study are in line with previous assessments of projected changes in heatwaves (Schleussner et al. 2016; Herrera-Estrada and Sheffield 2017; Russo 2017). The risks posed by short-term concurrent droughts and heatwaves would lead to more potential crop yield reductions in humid subtropical basins such as the Gan River Basin, which would be more serious in a 2.0 °C world than a 1.5 °C world. In conjunction with other development challenges, short-term concurrent droughts and heatwaves represent a crucial challenge for regional food security, especially in developing countries with large populations.

Short-term meteorological variables are considered an important factor in drought and heatwave concurrences ascharacterized by sunny skies, strong short-wave solar radiation, high temperatures, low precipitation, and other phenomena (Otkin et al. 2013). A small amount of low-level cloud cover plus lengthy sunshine duration and high surface net solar radiation create excessive surface energy, which is transferred largely into the atmosphere via sensible and latent heat fluxes; these fluxes heat the atmosphere and increase the local air temperature. Water vapor flux divergence anomalies also tend to be positive, which makes effective precipitation rare. These atmospheric conditions altogether provide favorable conditions for concurrent droughts and heatwaves. Other atmospheric factors may also play important roles: for example, convective inhibition energy has a strong negative effect on precipitation and soil moisture (i.e., strong convective inhibition energy suppresses precipitation) (Myoung and Nielsengammon 2010).

Short-term evapotranspiration demand is a key factor affecting concurrent droughts and heatwaves. For given adequate soil moisture, high temperatures (heat waves) cause evapotranspiration anomalies (energy-limited evapotranspiration) to increase, which in turn deplete soil moisture to drop to drought levels. Persistence of precipitation deficit conditions can force a transition from energy-limited evapotranspiration to water-limited evapotranspiration, leading to decline in soil moisture and evapotranspiration anomalies (Otkin et al. 2017). More surface sensible heat fluxes are transferred to the near-surface atmosphere to further increase air temperatures. These land–atmosphere interactions altogether cause the Bowen ratio to increase (Mo and Lettenmaier 2016; Qian et al. 2017), creating conditions within which concurrent droughts and heatwaves are likely.

Global warming may increase the prevalence of short-term concurrent droughts and heatwaves if current precipitation levels do not change (Aghakouchak et al. 2015). In addition to elevated temperatures, the strengthened interdependence between temperature and precipitation may exacerbate the increase in concurrent droughts and heatwaves (Zscheischler and Seneviratne 2017). Local-scale concurrent events are often embedded within larger-scale systems, which in turn are affected by planetary-scale characteristics such as shifts in the radiation balance and associated changes in temperatures and location of the jet stream (Zscheischler et al. 2018).

5 Conclusions

This study was conducted to establish an initial assessment of short-term concurrent drought and heatwave projections using the downscaled CMIP5 outputs coupled with VIC

model in a humid subtropical basin. We focused on changes in concurrent events at 1.5 and 2.0 °C of global warming levels in terms of temporal and spatial characteristics. The findings presented here may provide a feasible scientific basis for the concurrent events adaptation and mitigation strategies tailored to specific global warming thresholds. Our conclusions can be summarized as follows:

1. By comparison against previously published data, our VIC model reliably simulates soil moisture and evapotranspiration in the Gan River Basin. Short-term concurrent events (HWCE and PDCE events) were precisely defined to demonstrate that combinations of multiple events that are not extremes at the individual level indeed can create an extreme event when combined.
2. The global average surface temperature anomaly reaches 1.5 °C above the pre-industrial level in the year 2024 under the RCP8.5 scenario and 2027 under RCP4.5; it arrives at 2.0 °C in the year 2038 under both RCP8.5 and 2047 in RCP4.5. The average warming is 0.32 °C (0.56 °C) higher in China than the global warming level of 1.5 °C (2.0 °C). Warming in the Gan River Basin is relatively close to the global average level.
3. The annual pentads of future concurrent events in the Gan River Basin present an increase with respect to the reference period. Under the RCP8.5 scenario, the medians of HWCE increased at a rate of 0.19 pentads/decade from 2006 to 2099 while PDCE medians increased by 0.4 pentads/decade. Under the RCP4.5 scenario, the medians of HWCE increased at a rate of 0.08 pentads/decade from 2006 to 2099 and PDCE medians by 0.11 pentads/decade. The uncertainty of concurrent events encompasses a wider range as global temperature increases. Future (2006–2099) HWCE FOCs in the southernmost reaches of the basin increase obviously and decrease from south to north with respect to the reference period. PDCE FOCs increase to relatively little extent in the central parts of the basin and to greater extent in the northern and southern parts of the basin. The future increases in historical low-value areas are greater than those of historical high-value regions in the spatial FOCs of concurrent events across the Gan River Basin.
4. Compared to the reference period, both types of concurrent events increase by more than 50% in the most parts of the basin whether there is 1.5 or 2.0 °C of global warming; the 0.5 °C difference from 1.5 to 2.0 °C accounts for around 20% of this increase. There are substantial increases (> 80% in HWCE and > 50% in PDCE) in historical low-value areas (< 1.5 pentads in HWCE and < 3.0 pentads in PDCE) in both types of concurrent events at a 1.5 or 2.0 °C world. These increases are especially pronounced for HWCEs in a 2.0 °C world. Maximum increases of > 60% were observed in HWCEs and > 90% in PDCEs in the 25th percentile values with both 1.5 and 2.0 °C of global warming, respectively. The climatological median pentads of concurrent events would likely be 9.6–17.6% less frequent in a 1.5 °C world than a 2.0 °C world.

Acknowledgements This study was jointly supported by the National Key R&D Program of China (2017YFA0603804), National Natural Science Foundation (41771069), Jiangsu Natural Science Funds for Distinguished Young Scholar "BK20140047", the Priority Academic Program Development of Jiangsu Higher Education Institutions (PAPD), and the Research and Innovation Project for College Graduates of Jiangsu Province (no. 1344051501007). Climate scenarios used were from the NEX-GDDP dataset prepared by the Climate Analytics Group and NASA Ames Research Center using the NASA Earth Exchange, and distributed by the NASA Center for Climate Simulation (NCCS).

References

Aghakouchak A, Cheng L, Mazdiyasni O, Farahmand A (2015) Global warming and changes in risk of concurrent climate extremes: insights from the 2014 California drought. Geophys Res Lett 41:8847–8852

Chen L, Frauenfeld OW (2014) Surface air temperature changes over the twentieth and twenty-first centuries in China simulated by 20 CMIP5 models. J Clim 27:3920–3937

Ford TW, Mcroberts DB, Quiring SM, Hall RE (2015) On the utility of in situ soil moisture observations for flash drought early warning in Oklahoma, USA. Geophys Res Lett 42:9790–9798

Good P, Booth BBB, Chadwick R, Hawkins E, Jonko A, Lowe JA (2016) Large differences in regional precipitation change between a first and second 2 K of global warming. Nat Commun 7:13667. https://doi.org/10.1038/ncomms13667

Hare B, Roming N, Schaeffer M, Schleussner C-F (2016) Implications of the 1.5 °C limit in the Paris Agreement for climate policy and decarbonisation. Clim Anal. Available at http://climateanalytics.org/files/1p5_australia_report_ci.pdf

Herrera-Estrada JE, Sheffield J (2017) Uncertainties in future projections of summer droughts and heat waves over the contiguous United States. J Clim 30:6225–6246

Huang J, Yu H, Dai A, Wei Y, Kang L (2017) Drylands face potential threat under 2 °C global warming target. Nat Clim Change. https://doi.org/10.1038/NCLIMATE3275

IPCC (2012) Managing the risks of extreme events and disasters to advance climate change adaptation. Special report of working groups I and II of the intergovernmental panel on climate change. Cambridge University Press, Cambridge

IPCC (2013) Climate change 2013: the physical science basic. Contribution of working group I to the fifth assessment report of the intergovernmental panel on climate change. Cambridge University Press, Cambridge

Jiang Z, Li W, Xu J, Li L (2015) Extreme precipitation indices over China in CMIP5 models. Part I: model evaluation. J Clim 28:8603–8619

Kebede H, Fisher DK, Young LD (2012) Determination of moisture deficit and heat stress tolerance in corn using physiological measurements and a low-cost microcontroller-based monitoring system. J Agron Crop Sci 198:118–129

King AD, Karoly DJ, Henley BJ (2017) Australian climate extremes at 1.5 °C and 2 °C of global warming. Nat Clim Change. https://doi.org/10.1038/NCLIMATE3296
Kintisch E (2014) Is Atlantic holding Earth's missing heat? Science 345:860–861
Knutti R, Sedláček J (2013) Robustness and uncertainties in the new CMIP5 climate model projections. Nat Clim Change 3:369–373
Knutti R, Rogelj J, Sedláček J, Fischer EM (2015) A scientific critique of the two-degree climate change target. Nat Geosci 9:13–19. https://doi.org/10.1038/NGEO2595
Kraaijenbrink PDA, Bierkens MFP, Lutz AF, Immerzeel WW (2017) Impact of a global temperature rise of 1.5 degrees Celsius on Asia's glaciers. Nature 549:257–260
Mazdiyasni O, Aghakouchak A (2015) Substantial increase in concurrent droughts and heatwaves in the United States. Proc Natl Acad Sci USA 112:11484–11489
Meinshausen M, Smith SJ, Calvin K, Daniel JS, Kainuma M, Lamarque J, Matsumoto K, Montzka S, Raper S, Riahi K (2011) The RCP greenhouse gas concentrations and their extensions from 1765 to 2300. Clim Change 109:213–241
Meinshausen M, Vogel E, Nauels A, Lorbacher K, Meinshausen N, Etheridge DM, Fraser PJ, Montzka SA, Rayner PJ, Trudinger CM (2017) Historical greenhouse gas concentrations for climate modelling (CMIP6). Geosci Model Dev 10:2057–2116
Mitchell D, James R, Forster PM, Betts RA, Shiogama H, Allen M (2016) Realizing the impacts of a 1.5 °C warmer world. Nat Clim Change 6:735–737
Mitchell D, AchutaRao K, Allen M, Bethke I, Beyerle U, Ciavarella A, Forster PM, Fuglestvedt J, Gillett N, Haustein K (2017) Half a degree additional warming, prognosis and projected impacts (HAPPI): background and experimental design. Geosci Model Dev 10:571–583
Mo KC, Lettenmaier DP (2015) Heat wave flash droughts in decline. Geophys Res Lett 42:2823–2829
Mo KC, Lettenmaier DP (2016) Precipitation deficit flash droughts over the United States. J Hydrometeorol 17:1169–1184
Myoung BS, Nielsengammon JW (2010) The convective instability pathway to warm season drought in Texas. Part I: the role of convective inhibition and its modulation by soil moisture. J Clim 23:4461–4473
Nasrollahi N, AghaKouchak A, Cheng L, Damberg L, Thomas JP, Miao C, Hsu K, Sorooshian S (2015) How well do CMIP5 climate simulations replicate historical trends and patterns of meteorological droughts? Water Resour Res 51:2847–2864
Otkin JA, Anderson MC, Hain C, Mladenova IE, Basara JB, Svoboda M (2013) Examining rapid onset drought development using the thermal infrared-based evaporative stress index. J Hydrometeorol 14:1057–1074
Otkin JA, Anderson MC, Hain C, Svoboda M, Johnson D, Mueller R, Tadesse T, Wardlow B, Brown J (2016) Assessing the evolution of soil moisture and vegetation conditions during the 2012 United States flash drought. Agric For Meteorol 218:230–242
Otkin JA, Svoboda M, Hunt ED, Ford TW, Anderson MC, Hain C, Basara JB (2017) Flash droughts: a review and assessment of the challenges imposed by rapid onset droughts in the United States. Bull Am Meteorol Soc. https://doi.org/10.1175/BAMS-D-1117-0149.1171
Paimazumder D, Done JM (2016) Potential predictability sources of the 2012 U.S. drought in observations and a regional model ensemble. J Geophys Res Atmos 121:12581–12592
Palazzi E, Hardenberg JV, Terzago S, Provenzale A (2015) Precipitation in the Karakoram-Himalaya: a CMIP5 view. Clim Dyn 45:21–45
Qian Y, Hsu P-C, Cheng C-H (2017) Changes in surface energy partitioning in China over the past three decades. Adv Atmos Sci 34:635–649
Rodell M, Houser P, Jambor U, Gottschalck J, Mitchell K, Meng C, Arsenault K, Cosgrove B, Radakovich J, Bosilovich M (2004) The global land data assimilation system. Bull Am Meteorol Soc 85:381–394
Russo S (2017) Humid heat waves at different warming levels. Sci Rep 7:7477. https://doi.org/10.1038/s41598-41017-07536-41597
Russo S, Dosio A, Graversen RG, Sillmann J, Carrao H, Dunbar MB, Singleton A, Montagna P, Barbola P, Vogt JV (2015) Magnitude of extreme heat waves in present climate and their projection in a warming world. J Geophys Res Atmos 119:12500–512512
Schleussner C-F, Lissner TK, Fischer EM, Wohland J, Perrette M, Golly A, Rogelj J, Childers K, Schewe J, Frieler K, Mengel M, Hare W, Schaeffer M (2016) Differential climate impacts for policy-relevant limits to global warming: the case of 1.5 °C and 2 °C. Earth Syst Dyn 7:327–351
Schleussner CF, Pfleiderer P, Fischer EM (2017) In the observational record half a degree matters. Nat Clim Change 7:460–462
Sharma D, Babel MS (2013) Application of downscaled precipitation for hydrological climate-change impact assessment in the upper Ping River Basin of Thailand. Clim Dyn 41:2589–2602
Sharma S, Mujumdar P (2017) Increasing frequency and spatial extent of concurrent meteorological droughts and heatwaves in India. Sci Rep 7:15582
Svoboda M, Lecomte D, Hayes M, Heim R, Gleason K, Angel J, Rippey B, Tinker R, Palecki M, Stooksbury D (2002) The drought monitor. Bull Am Meteorol Soc 83:1181–1190
Tao H, Fraedrich K, Menz C, Zhai J (2014) Trends in extreme temperature indices in the Poyang Lake Basin, China. Stoch Env Res Risk Assess 28:1543–1553
Taylor KE, Stouffer RJ, Meehl GA (2012) An overview of CMIP5 and the experiment design. Bull Am Meteorol Soc 93:485–498
Thrasher B, Maurer EP, Mckellar C, Duffy PB (2012) Technical Note: bias correcting climate model simulated daily temperature extremes with quantile mapping. Hydrol Earth Syst Sci 16:3309–3314
United Nations Framework Convention on Climate Change (2015) Adoption of the paris agreement. ReportNo. FCCC/CP/2015/L.9/Rev.1. Available at http://unfccc.int/resource/docs/2015/cop21/eng/l09r01.pdf
Venkataraman K, Tummuri S, Medina A, Perry J (2016) 21st century drought outlook for major climate divisions of Texas based on CMIP5 multimodel ensemble: implications for water resource management. J Hydrol 534:300–316
Wang L, Yuan X, Xie Z, Wu P, Li Y (2016) Increasing flash droughts over China during the recent global warming hiatus. Sci Rep 6:30571
Wang Z, Lin L, Zhang X, Zhang H, Liu L, Xu Y (2017) Scenario dependence of future changes in climate extremes under 1.5 °C and 2 °C global warming. Sci Rep 7:46432. https://doi.org/10.41038/srep46432
Woznicki SA, Nejadhashemi AP, Tang Y, Wang L (2016) Large-scale climate change vulnerability assessment of stream health. Ecol Ind 69:578–594
You Q, Fraedrich K, Sielmann F, Min J, Kang S, Ji Z, Zhu X, Ren G (2014) Present and projected degree days in China from observation, reanalysis and simulations. Clim Dyn 43:1449–1462
You Q, Jiang Z, Kong L, Wu Z, Bao Y, Kang S, Pepin N (2017) A comparison of heat wave climatologies and trends in China based on multiple definitions. Clim Dyn 48:3975–3989
Yuan X, Wang L, Wood EF (2018) Anthropogenic intensification of Southern african flash droughts as exemplified by the 2015/16 season. Bull Am Meteorol Soc 99:S86–S90
Zhang X-J, Tang Q, Pan M, Tang Y (2014) A long-term land surface hydrologic fluxes and states dataset for China. J Hydrometeorol 15:2067–2084

Zhang Z, Chen X, Xu CY, Hong Y, Hardy J, Sun Z (2015) Examining the influence of river–lake interaction on the drought and water resources in the Poyang Lake basin. J Hydrol 522:510–521

Zhang Y, You Q, Chen C, Ge J (2016) Impacts of climate change on streamflows under RCP scenarios: a case study in Xin River Basin, China. Atmos Res 178:521–534

Zhang Y, You Q, Chen C, Xin L (2017a) Flash droughts in a typical humid and subtropical basin: a case study in the Gan River Basin, China. J Hydrol 551:162–176

Zhang Y, You Q, Ye L, Chen C (2017b) Spatio-temporal variability and possible mechanism of rainy season precipitation in Poyang Lake Basin, China. Clim Res 72:129–140

Zhang Y, You Q, Chen C, Ge J, Adnan M (2018) Evaluation of downscaled CMIP5 coupled with VIC model in simulating flash droughts in a humid subtropical basin, China. J Clim 31:1075–1090

Zscheischler J, Seneviratne SI (2017) Dependence of drivers affects risks associated with compound events. Sci Adv 3:e1700263

Zscheischler J, Westra S, Hurk BJ, Seneviratne SI, Ward PJ, Pitman A, AghaKouchak A, Bresch DN, Leonard M, Wahl T (2018) Future climate risk from compound events. Nat Clim Change 8:469–477. https://doi.org/10.1038/s41558-018-0156-3